Dopamine release in nucleus accumbens is under tonic inhibition by adenosine A_1 receptors regulated by astrocytic ENT1 and dysregulated by ethanol

Bradley M. Roberts[1,2], Elizabeth Lambert[1], Jessica A. Livesey[1], Zhaofa Wu[3], Yulong Li[3] & Stephanie J. Cragg[1,2]

[1] Centre for Integrative Neuroscience, Department of Physiology, Anatomy and Genetics, University of Oxford, Oxford OX1 3PT, United Kingdom
[2] Oxford Parkinson's Disease Centre, University of Oxford, Oxford OX1 3PT, United Kingdom
[3] State Key Laboratory of Membrane Biology, Peking University School of Life Sciences, Beijing, China

Corresponding authors: Professor Stephanie Cragg
Email: Stephanie.Cragg@dpag.ox.ac.uk
Dr Bradley Roberts
Email: Bradley.Roberts@dpag.ox.ac.uk

Abbreviated title: Tonic A_1R-inhibition of NAcC dopamine release

Manuscript length: Abstract (250 words), Significance Statement (119 words), Introduction (638 words), and Discussion (1,636 words); Main Figures (6); Tables (1)

Author contributions: B.M.R. and S.J.C. conceived and designed the research, and wrote the manuscript with input from all other authors; B.M.R. and E.L. assisted in the collection, analysis and interpretation of voltammetry data; B.M.R. and J.A.L. assisted in the collection, analysis and interpretation of adenosine GRAB imaging data; Y.L. and Z.W. conceived of, designed, and provided Adenosine GRAB construct.

Acknowledgements: This work was supported by grants from the UK Medical Research Council (MR/V013599/1 to S.J.C. and B.M.R.) and the University of Oxford John Fell Fund (0008310 to B.M.R.), a Junior Research Fellowship to B.M.R from St John's College, Oxford, and a BBSRC Doctoral Training Grant to J.A.L.

Conflict of interest: The authors declare no competing financial interests associated with this study.

ABSTRACT (250 words)

Striatal adenosine A_1 receptor (A_1R) activation can inhibit dopamine release. A_1Rs on other striatal neurons are activated by an adenosine tone that is limited by equilibrative nucleoside transporter 1 (ENT1) that is enriched on astrocytes and is ethanol-sensitive. We explored whether dopamine release in nucleus accumbens core is under tonic inhibition by A_1Rs, and is regulated by astrocytic ENT1 and ethanol. In *ex vivo* striatal slices from male and female mice, A_1R agonists inhibited dopamine release evoked electrically or optogenetically and detected using fast-scan cyclic voltammetry, most strongly for lower stimulation frequencies and pulse numbers, thereby enhancing the activity-dependent contrast of dopamine release. Conversely, A_1R antagonists reduced activity-dependent contrast but enhanced evoked dopamine release levels, even for single optogenetic pulses indicating an underlying tonic inhibition. The ENT1 inhibitor NBTI reduced dopamine release and promoted A_1R-mediated inhibition, and conversely, virally-mediated astrocytic overexpression of ENT1 enhanced dopamine release and relieved A_1R-mediated inhibition. By imaging the genetically encoded fluorescent adenosine sensor GRAB-Ado, we identified a striatal extracellular adenosine tone that was elevated by the ENT1 inhibitor and sensitive to gliotoxin fluorocitrate. Finally, we identified that ethanol (50 mM) promoted A_1R-mediated inhibition of dopamine release, through diminishing adenosine uptake via ENT1. Together, these data reveal that dopamine output dynamics are gated by a striatal adenosine tone, limiting amplitude but promoting contrast, regulated by ENT1, and promoted by ethanol. These data add to the diverse mechanisms through which ethanol modulates striatal dopamine, and to emerging datasets supporting astrocytic transporters as important regulators of striatal function.

SIGNIFICANCE STATEMENT (119 words)

Dopamine axons in the mammalian striatum are emerging as strategic sites where neuromodulators can powerfully influence dopamine output in health and disease. We found that ambient levels of the neuromodulator adenosine tonically inhibit dopamine release in nucleus accumbens core via adenosine A_1 receptors (A_1Rs), to a variable level that promotes the contrast in dopamine signals released by different frequencies of activity. We reveal that the equilibrative nucleoside transporter 1 (ENT1) on astrocytes limits this tonic inhibition, and that ethanol promotes it by diminishing adenosine uptake via ENT1. These findings support the hypotheses that A_1Rs on dopamine axons inhibit DA release and, furthermore, that astrocytes perform important roles in setting the level of striatal dopamine output, in health and disease.

INTRODUCTION (638 words)

Striatal dopamine (DA) axons are major strategic sites for striatal neuromodulators to influence DA output (Nolan et al., 2020; Rice et al., 2011; Roberts et al., 2021; Sulzer et al., 2016). Adenosine acts at A_1- and A_{2A}-receptors on diverse neurons in striatum, and exogenous activation of striatal A_1-receptors (A_1Rs) but not A_2-receptors inhibits evoked DA release (Okada et al., 1996; O'Neill et al., 2007; O'Connor and O'Neill, 2008; Ross and Venton, 2015). Immunocytochemical studies of rat synaptosomes suggest that A_1Rs can be localised directly to striatal DA axons (Borycz et al., 2007), but definitive evidence is lacking and other intermediary inputs to DA axons have not been excluded. In nucleus accumbens core (NAcC), adenosine can provide tonic A_1R-mediated inhibition of glutamatergic and GABAergic transmission (Brundege and Williams, 2002; Adhikary and Birdsong, 2021). DA release in NAcC and caudate-putamen has been suggested to be under tonic A_1R-mediated inhibition, as A_1R antagonists increase extracellular DA levels in rats *in vivo* measured by microdialysis (Okada et al., 1996; Solinas et al., 2002; Quarta et al., 2004a, 2004b; Borycz et al., 2007), but whether these effects were direct and local, or involved intact long-loop circuits was not resolved. Furthermore, adenosine acts in a frequency-dependent manner on glutamate and GABA transmission across other nuclei, resulting in a stronger A_1R-dependent inhibition of neurotransmission elicited by low-frequency versus high-frequency electrical stimulations (e.g. neocortex: Perrier et al., 2019; Qi et al., 2017; Yang et al., 2007; hippocampus: Moore et al., 2003; calyx of Held: Wong et al., 2006). It has not yet been established whether striatal A_1Rs simply inhibit DA neurotransmission, or might also promote contrast in DA signals released by different firing rates, and whether in turn this is independent from striatal acetylcholine or GABA circuits which modify DA signal contrast (Rice and Cragg, 2004; Lopes et al., 2019).

Extracellular adenosine concentrations are limited by the activity of nucleoside transporters, most notably the equilibrative nucleoside transporter type 1 (ENT1) (Young et al., 2008; Nguyen et al., 2015). ENT1 is expressed in striatum (Jennings et al., 2001; Anderson et al., 2002) and is especially abundant on astrocytes (Peng et al., 2005; Chai et al., 2017). ENT1 on astrocytes can regulate adenosine signalling in striatum and elsewhere (Nagai et al., 2005; Tanaka et al., 2011; Boddum et al., 2016; Cheffer et al., 2018; Hong et al., 2020), and in dorsal striatum, astrocytic ENT1 activity modulates reward-seeking behaviours (Hong et al., 2020; Kang et al., 2020). We recently identified that astrocytes regulate DA release, owing to their expression of GABA transporters that regulate tonic GABAergic inhibition (Roberts et al., 2020), but whether ENT1 on astrocytes also modulates DA output by regulating adenosine tone at A_1Rs has not been explored. Additionally, adenosine uptake by ENT1 is impaired by acute ethanol, which augments extracellular adenosine levels (Nagy et al., 1989, 1990; Choi et al., 2004) and contributes to the ataxic and hypnotic effects of ethanol through activation of striatal A_1Rs (Meng and Dar, 1995; Phan et al., 1997; Dar, 2001). Acute ethanol reduces DA release evoked in NAcC in brain slices (Yorgason et al., 2014, 2015), as does chronic intermittent ethanol exposure in mice (Karkhanis et al., 2015; Rose et al., 2016), raising the question of whether ethanol regulates DA by promoting A_1R-mediated inhibition of DA release.

Here, we assessed A_1R regulation of DA release in NAcC by detecting DA in real-time using fast-scan cyclic voltammetry and detecting striatal adenosine using the genetically encoded fluorescent adenosine sensor (GRAB-Ado) (Peng et al., 2020; Wu et al., 2020). We reveal that A_1Rs can tonically inhibit DA output though an ambient adenosine tone, and that A_1Rs additionally regulate the activity-sensitivity of DA release, independently from striatal acetylcholine or GABA inputs. Furthermore, we find that tonic A_1R-mediated inhibition of DA release is regulated by adenosine uptake by ENT1 on astrocytes, and dysregulated by ethanol.

MATERIALS & METHODS

Animals

All procedures were performed in accordance with the Animals in Scientific Procedures Act 1986 (Amended 2012) with ethical approval from the University of Oxford, and under authority of a Project Licence granted by the UK Home Office. Experiments were carried out using male and female adult (6−12 week-old) C57BL/6J mice (Charles River) or heterozygote knock-in mice bearing an internal ribosome entry site (IRES)-linked Cre recombinase gene downstream of the gene *Slc6a3*, which encodes the plasma membrane DA transporter (*Slc6a3*$^{IRES\text{-}Cre}$ mice; *B6.SJL-Slc6a3*$^{tm1.1(cre)Bkmn}$/J; Jackson Laboratories stock no. 006660) maintained on a C57BL/6J background. All mice were group-housed and maintained on a 12-hr light cycle (light ON from 07:00 – 19:00) with *ad libitum* access to food and water. Data from male and female mice were combined throughout as no differences in the effects of adenosine A_1 receptor agonists or antagonists between sexes were observed (**Table 1**).

Stereotaxic intracranial injections

Mice were anesthetized with isoflurane and placed in a small animal stereotaxic frame (David Kopf Instruments). After exposing the skull under aseptic techniques, a small burr hole was drilled and adeno-associated viral solutions were injected at an infusion rate of 100 nL/min with a 32-gauge Hamilton syringe (Hamilton Company) using a microsyringe pump (World Precision Instruments) and withdrawn 5 min after the end of injection. To virally express ChR2 selectively in DA neurons, 600 nL per hemisphere of AAV5-EF1α-DIO-hChR2(H134R)-eYFP (8×10^{12} genome copies per ml; UNC Vector Core Facility) encoding Cre-dependent ChR2 was injected bilaterally into the midbrain (AP −3.1 mm, ML ± 1.2 mm from bregma, DV −4.25 mm from exposed dura mater) of 6 week-old *Slc6a3*$^{IRES\text{-}Cre}$ mice, following previously described methods (Roberts et al., 2020). To overexpress ENT1 in striatal astrocytes, 600 nL per hemisphere of AAV5-GfaABC$_1$D-mENT1/mCherry-WPRE (1.6×10^{13} genome copies per ml; Vector Biolabs) encoding a fluorescence protein-fused and functional ENT1 under the astrocyte-specific abbreviated glial fibrillary acidic protein promoter (*GfaABC$_1$D*) (Hong et al., 2020; Jia et al., 2020) or AAV5-GfaABC$_1$D-mCherry-WPRE (6.1×10^{12} genome copies per ml; ETH Zurich Viral Vector Facility) for control fluorophore expression, was injected bilaterally into nucleus accumbens (AP +1.3 mm, ML ± 1.2 mm from bregma, DV −3.75 mm from exposed dura mater) of 6 week-old C57BL/6J wild-type mice. To virally express the fluorescent adenosine reporter GRAB-Ado (Peng et al., 2020; Wu et al., 2020), 800 nL per hemisphere of AAV9-hSyn-GRAB-Ado1.0m (0.5×10^{13} genome copies per ml; WZ Biosciences) was injected

bilaterally into nucleus accumbens or dorsal striatum (AP +0.8 mm, ML ± 1.75 mm from bregma, DV −2.40 mm from exposed dura mater) of 6 week-old C57BL/6J wild-type mice. Mice were used for experiments 2−4 weeks post-intracranial injection.

Brain slice preparation

Acute brain slices were obtained from 8 – 12-week-old mice using standard techniques. Mice were culled by cervical dislocation within 1 – 2 hrs after start of light ON period of light cycle and brains were dissected out and submerged in ice-cold cutting solution containing (in mM): 194 sucrose, 30 NaCl, 4.5 KCl, 1 $MgCl_2$, 26 $NaHCO_3$, 1.2 NaH_2PO_4, and 10 D-glucose. Coronal slices 300 µm-thick containing striatum were prepared from dissected brain tissue using a vibratome (VT1200S, Leica Microsystems) and transferred to a holding chamber containing artificial cerebrospinal fluid (aCSF) containing (in mM): 130 NaCl, 2.5 KCl, 26 $NaHCO_3$, 2.5 $CaCl_2$, 2 $MgCl_2$, 1.25 NaH_2PO_4 and 10 glucose. Sections were incubated at 34 °C for 15 min before they were stored at room temperature (20–22 °C) until recordings were performed. All recordings were obtained within 8 h of slicing. All solutions were saturated with 95% O_2/5% CO_2. Before recording, individual slices were hemisected and transferred to a recording chamber and superfused at ~2.5–3.0 mL/min with aCSF at 31–33 °C.

Fast-scan cyclic voltammetry (FSCV)

Evoked extracellular DA concentration ($[DA]_o$) was measured in acute coronal brain slices using FSCV at carbon-fibre microelectrodes (7–10 µm diameter) fabricated in-house (tip length 70–120 µm) as used previously (Roberts et al., 2020). In brief, a triangular voltage waveform was scanned across the microelectrode (−700 to +1300 mV vs Ag/AgCl reference) at 800 V/s and at a scan frequency of 8 Hz using a Millar Voltammeter (Julian Millar, Barts and the London School of Medicine and Dentistry). Microelectrodes were calibrated post-hoc in 2 µM DA in each experimental solution. Microelectrode sensitivity to DA was between 10 and 40 nA/µM. Signals were attributed to DA due to the potentials of their characteristic oxidation (500-600 mV) and reduction (−200 mV) peaks. Currents at the oxidation peak potential were measured from the baseline of each voltammogram and plotted against time to provide profiles of $[DA]_o$ versus time. Recordings were carried out in the nucleus accumbens core (NAcC), within ~100 µm of the anterior commissure, one site per slice. Electrical or light stimuli were delivered at 2.5 min intervals, which allow stable DA release to be sustained at ~90–95% of original levels over the typical time course of experiments, in control conditions (Roberts et al., 2020). In experiments where $[DA]_o$ was evoked by electrical stimulation, a local bipolar concentric Pt/Ir electrode (25 µm inner diameter, 125 µm outer diameter; FHC Inc.) was placed ~100 µm from the recording microelectrode and stimulus pulses (200 µs duration) were given at 0.6 mA. We applied either single pulses (1p) or trains of 2–20 pulses at 10–100 Hz. In experiments where $[DA]_o$ was evoked by light stimulation in slices prepared from *Slc6a3*$^{IRES\text{-}Cre}$ mice expressing ChR2, DA axons in striatum were activated by TTL-driven (Multi Channel Stimulus II, Multi Channel Systems) brief pulses (2 ms) of blue light (470 nm; 5 $mWmm^{-2}$; OptoLED, Cairn Research), which illuminated the field of view (2.2 mm diameter, ×10 water-immersion objective). Data were digitized at 50 kHz using a Digidata 1550A digitizer (Molecular Devices). Data were acquired and analysed using Axoscope 11.0 (Molecular Devices) and locally written VBA scripts in Microsoft Excel (2013).

GRAB-Ado Imaging

An Olympus BX51WI microscope equipped with a 470 nm OptoLED light system (Cairn Research), Iris 9 Scientific CMOS camera (Teledyne Photometrics), 525/50 nm emission filter (Cairn Research), and x10/0.3 NA water-immersion objective (Olympus) was used for wide-field fluorescence imaging of GRAB-Ado in striatal slices. Images acquisition was controlled using Micro-Manager 1.4. Electrical stimulations, LED light, and image acquisition were synchronised using TTL-driven stimuli via Multi Channel Stimulus II (Multi Channel Systems). Image files were analysed with Matlab R2017b and Fiji 1.5. For experiments measuring changes to basal, non-stimulated extracellular adenosine levels, images (100 ms exposure duration) were acquired every 30 s during brief exposure (1 s) to blue light (470 nm; 1 $mWmm^{-2}$; OptoLED, Cairn Research) for a 40 min window. We extracted fluorescence intensity from the region of interest (ROI; 150 x 150 µm) and derived a background-subtracted fluorescence intensity (F_t) by subtracting background fluorescence intensity from an equal-sized ROI where there was no GRAB-Ado expression (i.e. cortex). Data are expressed as a change in fluorescence ($\Delta F/F_0$) and were derived by calculating $[(F_t-F_0)/F_0]$, where F_0 is the average background-subtracted fluorescence intensity (F_t) of the first 20 acquired images (initial 10 mins). For experiments measuring extracellular adenosine levels in response to trains of electrical stimulation or experiments calibrating GRAB-Ado signals to applications of known concentrations of exogenous adenosine, images were acquired at 10 Hz (100 ms exposure duration) during continuous blue light (470 nm; 1 $mWmm^{-2}$; OptoLED, Cairn Research) for a 4 min recording window. For evoked adenosine release, electrical stimulus pulses (100 pulses at 50 Hz, 200 µs pulse duration, 0.6 mA) were given by a local bipolar concentric Pt/Ir electrode (25 µm inner diameter, 125 µm outer diameter; FHC Inc.) at the 30 second timepoint. Bath applications of exogenous adenosine were also applied at the 30 second timepoint. Background-subtracted fluorescence intensity (F_t) was extracted from an ROI (150 x 150 µm) ~50 µm from the stimulating electrode and $\Delta F/F_0$ was derived by calculating $[(F_t-F_0)/F_0]$, where F_0 is the average fluorescence intensity over the 10 s window (100 images) prior to onset of electrical stimulation or bath application of exogenous adenosine.

Drugs

Adenosine (Ado, 25-100 µM), (+)-bicuculline (10 µM), dihydro-β-erythroidine hydrobromide (DHβE, 1 µM), nitrobenzylthioinosine (NBTI, 10 µM), and tetrodotoxin (TTX, 1 µM) were obtained from Tocris Bioscience. CGP 55845 hydrochloride (CGP, 4 µM), 8-Cyclopentyl-1,3-dimethylxanthine (CPT, 10 µM), and dipropylcyclopentylxanthine (DPCPX, 2 µM) were obtained from Abcam. Ethanol (EtOH, 50 mM), and N^6-cyclopentyladenosine (CPA, 15 µM) were obtained from Sigma-Aldrich. Fluorocitrate (FC) was prepared as previously described (Paulsen et al., 1987; Roberts et al., 2020). In brief, D,L-fluorocitric acid Ba_3 salt (Sigma–Aldrich) was dissolved in 0.1 M HCl, the Ba^{2+} precipitated with 0.1 M Na_2S0_4 and then centrifuged at 1000 × g for 5 min. Supernatant containing fluorocitrate was used at a final concentration of 100 µM for experimentation.

Immunocytochemistry

To confirm viral ENT1-mCherry expression in non-neuronal cells, direct mCherry fluorophore expression was compared to indirect immunofluorescence for neuronal marker NeuN. ENT1-mCherry expressing mice were

anaesthetised with an overdose of pentobarbital and transcardially perfused with phosphate-buffered saline (PBS), followed by 4% paraformaldehyde in 0.1 M phosphate buffer, pH 7.4. Brains were removed and post-fixed overnight in 4% PFA. Coronal sections were cut using a vibrating microtome (Leica VT1000S) at a thickness of 50 µm and collected in a 1 in 4 series. Sections were stored in PBS with 0.05% sodium azide until processing. Upon processing, sections were washed in PBS and then blocked for 1 h in a solution of PBS TritonX (0.3%; PBS-Tx) containing 10% normal donkey serum (NDS). Sections were then incubated in primary antibodies overnight in PBS-Tx with 2% NDS at 4 °C. Primary antibodies: rabbit anti-NeuN (1:500, Biosensis, R-3770–100). Sections were then incubated in species-appropriate fluorescent secondary antibodies with minimal cross-reactivity for 2 hours in PBS-Tx with 2% NDS at room temperature. Secondary antibodies: Donkey anti-rabbit AlexaFluor 405 (1:500, Abcam, ab175651). Sections were washed in PBS and then mounted on glass slides and cover-slipped using Vectashield (Vector Labs). Coverslips were sealed using nail varnish and stored at 4 °C. Confocal images were acquired with an Olympus FV3000 Confocal Laser Scanning Microscope using a x20 and x40 objective and filters for appropriate excitation and emission wave lengths (Olympus Medical).

RESULTS

Adenosine A_1Rs inhibit striatal DA release

Previous studies have shown that agonists for striatal A_1Rs inhibit DA release evoked by discrete electrical stimulations in dorsal and ventral striatum (O'Neill et al., 2007; O'Connor and O'Neill, 2008; Ross and Venton, 2015). We firstly corroborated these observations in NAcC for DA release evoked by single stimulus pulses and detected using FSCV in *ex vivo* coronal slices (**Figure 1A**). Bath application of A_1R agonist CPA (15 µM) reduced evoked $[DA]_o$ by ~50% (**Figure 1B**, $t_{(5)} = 15.2$, $p < 0.0001$, paired t test). This effect of CPA was prevented by prior application of A_1R antagonist DPCPX (2 µM) (**Figure 1B**, $F_{(1, 11)} = 88.6$, $p < 0.0001$, two-way RM ANOVA for effect of CPA in the absence vs presence of DPCPX; **Figure 1E**, $t_{(11)} = 9.99$, $p < 0.0001$, unpaired t test), confirming an action via A_1Rs.

Striatal cholinergic interneurons (ChIs) have A_1Rs (Alexander and Reddington, 1989; Ferré et al., 1996; Song et al., 2000; Preston et al., 2009) through which A_1R agonists can hyperpolarise ChIs and inhibit ACh release (Richardson and Brown, 1987; Brown et al., 1990; Preston et al., 2009). Because ChIs operate strong control over DA release via nAChRs (Jones et al., 2001; Rice and Cragg, 2004; Zhang and Sulzer, 2004), and can mediate the effects of other striatal neuromodulators on DA (Britt and McGehee, 2008; Hartung et al., 2011; Stouffer et al., 2015; Kosillo et al., 2016; Lemos et al., 2019), they might indirectly mediate the control of DA by A_1Rs. We explored whether A_1Rs can modulate striatal DA release in the absence of these potential actions on ChIs and nAChRs. We used nAChR antagonist DHβE (1 µM) to inhibit nAChRs as described previously (Rice and Cragg, 2004; Threlfell et al., 2012), after which subsequent application of CPA nonetheless reduced evoked $[DA]_o$ evoked by single stimulus pulses by ~50% (**Figure 1C**, $t_{(4)} = 15.9$, $p < 0.0001$, paired t test), an effect not different from that seen in the absence of DHβE (**Figure 1C**, $F_{(1, 9)} = 1.22$, $p = 0.29$, two-way RM ANOVA: main

effect of drug; **Figure 1E**, $t_{(9)} = 1.21$, $p = 0.259$, unpaired t test), indicating that A_1Rs can suppress DA release independently from any indirect effects via ChI inputs to nAChRs.

DA release throughout striatum is also under tonic inhibition by GABA through action at $GABA_A$ and $GABA_B$ receptors (Lopes et al., 2019; Roberts et al., 2020), and we tested whether A_1Rs require this GABA input to inhibit DA release. However, in the presence of $GABA_A$ and $GABA_B$ receptor antagonists, bicuculline (10 µM) and CGP 55845 (5 µM) respectively, the A_1R agonist CPA (15 µM) significantly reduced $[DA]_o$ evoked in NAcC by single electrical pulses by ~40% (**Figure 1D**, $t_{(4)} = 6.10$, $p = 0.0036$, paired t test), an effect that was not significantly different from that seen in the absence of GABA receptor antagonists (**Figure 1D**, $F_{(1, 9)} = 0.019$, $p = 0.892$, two-way RM ANOVA: main effect of drug; **Figure 1E**, $t_{(9)} = 0.259$, $p = 0.802$, unpaired t test), indicating that A_1 receptor agonists can inhibit DA release independently from indirect effects acting via striatal GABA modulation of DA.

To further test whether the inhibition of DA release by A_1Rs requires the co-activation of other striatal neuron types or inputs, we tested whether A_1Rs modulate DA release evoked optogenetically by targeted light activation of DA axons. Optogenetic activation of DA axons minimises the activation of other striatal neurons that occurs with non-selective electrical stimulation; optogenetically evoked DA release is independent of at least nAChR input (Threlfell et al., 2012; Melchior et al., 2015). We expressed ChR2-eYFP in DA neurons and axons in $Slc6a3^{IRES\text{-}Cre}$ mice using an established viral approach (**Figure 1F**) as we previously described (Roberts et al., 2020). CPA suppressed $[DA]_o$ evoked in NAcC by single brief (2 ms) blue light pulses (**Figure 1G**, $t_{(7)} = 16.2$, $p < 0.0001$, paired t test), indicating that A_1Rs can inhibit DA release independently from not just ChI input to nAChRs but also without requiring the coincident activation of inputs from other neuron types, suggesting that A_1R inhibition of DA release could be via direct action on DA axons, although actions via an unidentified tonically active input that is not GABA are possible.

Striatal A_1Rs enhance the frequency- and activity-sensitivity of DA release

Previous studies exploring whether striatal A_1Rs regulate DA release have predominantly focused on the effects on release evoked by single, discrete stimuli, and impact on release by the full range of physiological relevant frequencies has not been explored. Adenosine acts in a frequency-dependent manner on glutamate and GABA transmission in other brain nuclei, resulting in a stronger A_1R-dependent inhibition of neurotransmission elicited by low-frequency versus high-frequency electrical stimulations, and therefore operating like a high-pass input filter on neurotransmitter release (e.g. neocortex: Perrier et al., 2019; Qi et al., 2017; Yang et al., 2007; hippocampus: Moore et al., 2003; calyx of Held: Wong et al., 2006). Other inputs and mechanisms that inhibit DA release by single stimuli can also promote the frequency dependence of DA release e.g. GABA (Lopes et al., 2019; Roberts et al., 2020) consistent with a reduction in the initial release probability and a consequent relief of some short-term depression (Condon et al., 2019). Using optogenetic activation, we observed a sizeable enhancement in the 5p:1p ratio (for 25 Hz) of light-evoked $[DA]_o$ in the NAcC following application of CPA (**Figure 1H**, $t_{(7)} = 10.4$, $p < 0.0001$, paired t test), suggesting that striatal A_1Rs might promote the sensitivity of DA release to firing rate.

We used electrical stimulation to investigate the effects of A_1R activation on DA release across a full range of physiological DA neuron firing frequencies (1, 10, 50 and 100 Hz), with varying pulse numbers (5, 10, 15 and 20 p). These experiments were carried out in the presence of nAChR antagonist DHβE (1 μM) to eliminate the effects of ChIs which profoundly restrict the apparent frequency- and activity-sensitivity of evoked DA release (Rice and Cragg, 2004; Zhang and Sulzer, 2004). A_1R activation by CPA (15 μM) inhibited DA release inversely and significantly with stimulation frequency (**Figure 2A-B**, $F_{(3, 18)} = 53.9$, $p < 0.0001$, one-way RM ANOVA), such that CPA significantly increased the frequency-dependence of evoked DA release (**Figure 2C**, $F_{(1, 7)} = 38.2$, $p = 0.0005$, two-way RM ANOVA: main effect of drug; $F_{(3, 21)} = 23.0$, $p < 0.0001$, frequency x drug interaction). In addition, A_1R activation by CPA inhibited DA release in a manner that varied inversely with number of pulses in a train (50 Hz) (**Figure 2D-E**, $F_{(6, 24)} = 31.1$, $p < 0.0001$, one-way RM ANOVA) which significantly increased the pulse-dependence of evoked DA release (**Figure 2F**, $F_{(1, 7)} = 46.7$, $p = 0.0002$, two-way RM ANOVA: main effect of drug; $F_{(4, 28)} = 28.2$, $p < 0.0001$, pulse number x drug interaction). Therefore, striatal A_1R do not simply inhibit DA release, but have a dynamic outcome depending on activity, that promotes the contrast in DA signals released by different activity.

Adenosine operates a tonic inhibition on DA release

We next addressed whether A_1Rs provide an endogenous inhibition of DA release levels and support the contrast in DA signals released by different activity. Previous *in vivo* microdialysis studies indicate that endogenous adenosine might even exert a tonic A_1R-mediated inhibition of DA release, as systemic dosing or intrastriatal infusions of A_1R antagonists (as well as competitive A_1 and A_{2A} receptor antagonist caffeine (Solinas et al., 2002; Quarta et al., 2004b)), increase extracellular striatal DA levels (Okada et al., 1996; Quarta et al., 2004a; Borycz et al., 2007). These effects might involve indirect actions via long loop circuits that are intact *in vivo* that could modulate DA neuron firing in midbrain. We tested therefore whether endogenous inhibition of DA release by A_1Rs could be localised to the NAcC and whether it occurs without co-activation of other neurons, indicative of an tonic inhibition of DA release, by exploring the effects of A_1R antagonists on DA release in NAcC evoked either electrically or optogenetically in coronal striatal slices.

Application of the A_1R antagonist CPT (10 μM) significantly enhanced $[DA]_o$ evoked by single or five pulses (50 Hz) of electrical stimulation by ~30-40% (**Figure 3A**, 1p: $t_{(6)} = 5.10$, $p = 0.0022$; 5p: $t_{(6)} = 5.13$, $p = 0.0022$; paired t tests), and in turn, decreased the ratio of $[DA]_o$ evoked by 5p:1p (**Figure 3B**, $t_{(6)} = 3.72$, $p = 0.0099$, paired t test), indicative of an underlying regulation of DA release by endogenous adenosine. Caffeine (20 μM) also significantly enhanced $[DA]_o$ evoked by single or five pulses (50 Hz) of electrical stimulation by ~20-10% (**Figure 3C**; 1p: $t_{(5)} = 3.69$, $p = 0.014$; 5p: $t_{(5)} = 3.49$, $p = 0.018$; paired t tests) and decreased the ratio of $[DA]_o$ evoked by 5p:1p ratio (**Figure 3D**, $t_{(5)} = 3.59$, $p = 0.016$, paired t test). We then investigated whether A_1R-mediated inhibition of DA release by endogenous adenosine might arise through an ambient adenosine tone, by exploring whether A_1R antagonist CPT could promote DA release when evoked using optogenetic stimulation to activate DA axons selectively without co-activation of other striatal cell types that might provide a source of endogenous adenosine. CPT significantly enhanced $[DA]_o$ evoked by single and five pulses (25 Hz) of light in $Slc6a3^{IRES\text{-}Cre}$ ChR2-expressing mice by ~20-30% (**Figure 3E**, 1p: $t_{(7)} = 5.58$, $p = 0.0008$; 5p: $t_{(7)} = 5.51$, $p = 0.0009$;

paired t tests) and decreased the ratio of $[DA]_o$ evoked by 5p:1p (25 Hz) (**Figure 3F**, $t_{(7)} = 13.50$, $p < 0.0001$, paired t test). These data therefore suggest that striatal DA release is under tonic inhibition by an ambient adenosine tone at A_1Rs, which promotes contrast in DA signals released by different activity.

ENT1 on astrocytes is a regulator of tonic A_1R-mediated inhibition of DA release

We next tested the hypothesis that striatal ENT1 and, by association, astrocytes, by governing ambient adenosine levels (Nagai et al., 2005; Young et al., 2008; Tanaka et al., 2011; Nguyen et al., 2015; Cheffer et al., 2018; Hong et al., 2020), might determine the level of tonic A_1R-mediated inhibition of evoked DA release in NAcC. We first inhibited ENT1 activity by pre-treatment of slices with the selective ENT1 inhibitor NBTI (10 µM, for 45 – 60 min), which has previously been shown to increase adenosine levels in striatum (Pajski and Venton, 2010). ENT1 inhibition itself attenuated $[DA]_o$ evoked by single and five pulses (50 Hz) of electrical stimulation (**Figure 4A**; 1p: $t_{(12)} = 4.38$, $p = 0.0009$; 5p: $t_{(12)} = 3.02$, $p = 0.0107$; unpaired t tests). Furthermore, after pre-treatment with NBTI, the A_1R antagonist CPT (10 µM) enhanced $[DA]_o$ evoked by single electrical pulses to a significantly greater degree than in control slices (**Figure 4B**, $F_{(1, 12)} = 27.17$, $p = 0.0002$, two-way RM ANOVA: main effect of drug). CPT decreased the ratio of $[DA]_o$ evoked by 5p:1p (50 Hz) in both conditions (**Figure 4C**, $F_{(1, 12)} = 35.48$, $p < 0.0001$, two-way RM ANOVA: main effect of drug), but there was a significant statistical interaction between NBTI and CPT (**Figure 4C**, $F_{(1, 12)} = 9.48$, $p = 0.0096$, two-way RM ANOVA: NBTI x CPT interaction) borne out by a greater decrease in this ratio in slices pre-treated with NBTI compared to control slices (**Figure 4D**, $t_{(12)} = 3.08$, $p = 0.0096$, unpaired t test). These data suggest that ENT1 regulates, and in particular limits, how A_1 receptors tonically inhibit DA release and support its associated activity-sensitivity.

We then tested conversely whether an upregulation of ENT1 specifically on astrocytes could diminish the level of endogenous A_1R-mediated inhibition of DA release. We targeted fluorescence-tagged ENT1 to astrocytes in the NAcC (**Figure 4E-F**) using a viral approach already validated for striatal astrocytes (Hong et al., 2020; Jia et al., 2020). Astrocyte-targeted ENT1-overexpression (ENT1-OX) increased $[DA]_o$ evoked by single and five pulses (50 Hz) of electrical stimulation compared to targeted mCherry controls (**Figure 4G**, 1p: $t_{(15)} = 3.29$, $p = 0.0049$; 5p: $t_{(15)} = 3.49$, $p = 0.0033$; unpaired t tests). Furthermore, with ENT1-OX, the A_1R antagonist CPT (10 µM) enhanced $[DA]_o$ evoked by single electrical pulses to a significantly lesser degree than in mCherry controls (**Figure 4H**, $F_{(1, 15)} = 20.12$, $p = 0.0004$, two-way RM ANOVA: main effect of drug). CPT decreased the ratio of $[DA]_o$ evoked by 5p:1p (50 Hz) in ENT1-OX and mCherry controls (**Figure 4I**, $F_{(1, 15)} = 46.28$, $p < 0.0001$, two-way RM ANOVA: main effect of drug), but there was a significant statistical interaction between ENT1-OX and CPT (**Figure 4I**, $F_{(1, 15)} = 9.54$, $p = 0.0075$, two-way RM ANOVA: ENT1-OX x CPT interaction), which was borne out by a smaller decrease in this ratio following CPT application in ENT1-OX than in controls (**Figure 4J**, $t_{(15)} = 3.09$, $p = 0.0075$, unpaired t test). Together, these data suggest that ENT1 on astrocytes in particular can support adenosine uptake and set the level of inhibition and regulation of activity-dependence of DA release by ambient adenosine acting at A_1Rs.

To resolve directly whether ENT1, and astrocytes, govern striatal adenosine levels, we detected adenosine levels by imaging the recently developed GRAB-Ado sensor (Peng et al., 2020; Wu et al., 2020), a virally

expressed genetic reporter, injected into striatum (**Figure 5A**). We confirmed that striatal GRAB-Ado sensor fluorescence responded to adenosine concentrations in a concentration-dependent manner on application of exogenous adenosine to slices (**Figure 5B**, $F_{(3,35)} = 28.73$, $p < 0.0001$, one-way ANOVA), and with a large range of dF/F. To assess the impact of ENT1 on ambient adenosine tone in NAcC, we imaged GRAB-Ado fluorescence before and after ENT1 inhibition, in the absence of any stimulation. Bath application of ENT1 inhibitor NBTI (10 µM) increased fluorescence compared to vehicle controls (**Figure 5C**, $F_{(1,18)} = 57.8$, $p < 0.0001$, two-way RM ANOVA: main effect of NBTI), indicating that ENT1 limits extracellular adenosine levels. To test whether ENT1 on astrocytes participate in this mechanism, we tested whether metabolic inhibition of astrocytes limited ENT1 function. We pre-treated slices with the gliotoxin fluorocitrate (100 µM, for 45 – 60 min), which has been established to induce metabolic arrest in astrocytes, render them inactive and prevent the effects of astrocytic transporters (Paulsen et al., 1987; Henneberger et al., 2010; Bonansco et al., 2011; Boddum et al., 2016; Roberts et al., 2020). The effects of ENT1 inhibitor NBTI on GRAB-Ado fluorescence were occluded after pre-treatment with fluorocitrate (**Figure 5D**, $F_{(1,14)} = 14.32$, $p = 0.002$, two-way RM ANOVA: main effect of FC).

To further characterise and validate the role of ENT1 and astrocytes in striatal adenosine signalling, we explored their impact on the dynamics of extracellular adenosine transients evoked electrically by trains of electrical stimulation (100 pulses, 50 Hz) (**Figure 5E**). Evoked increases in extracellular adenosine concentrations exhibited relatively extended rise times (~30 sec) and clearance times as reported previously in cultured hippocampal neurons and acute hippocampal and medial prefrontal cortex mouse brain slices (Wu et al., 2020), and surprisingly release was activated via a mechanism that was not prevented by Na_v blocker TTX (1 µM). (**Figure 5E**, $F_{(3,29)} = 13.60$, $p < 0.0001$, one-way ANOVA; TTX vs control: $p > 0.99$, Sidak's multiple comparisons). In slices pre-treated with the ENT1 inhibitor NBTI (10 µM, for 45 – 60 min), the peak of evoked adenosine levels was attenuated (**Figure 5E**, $F_{(3,29)} = 13.60$, $p < 0.0001$, one-way ANOVA; NBTI vs control: $p = 0.001$, Sidak's multiple comparisons), but the clearance time constant was extended (**Figure 5F**, $F = 8543$, $p < 0.0001$, extra-sum-of-squares F test; control: $\tau = 108.4$, NBTI: $\tau = 564.5$), indicating reduced release and uptake, and seen previously in cultured hippocampal neurons (Wu et al., 2020). In slices pre-treated with the gliotoxin fluorocitrate (100 µM, for 45 – 60 min), both the peak level of adenosine and the time constant for clearance were elevated (**Figure 5E**, $F_{(3,29)} = 13.60$, $p < 0.0001$, one-way ANOVA; FC vs control: $p = 0.049$, Sidak's multiple comparisons; **Figure 5F**, $F = 8543$, $p < 0.0001$, extra-sum-of-squares F test; control: $\tau = 108.4$, FC: $\tau = 217.0$), indicating that ENT1 on astrocytes support adenosine uptake

EtOH increases tonic A_1R-mediated inhibition of DA release

Our data indicate that astrocytic ENT1 function regulates tonic A_1R-mediated inhibition of DA output in NAcC. Acute exposure to ethanol is documented to increase extracellular adenosine levels in many brain nuclei, including striatum, via inhibition of adenosine uptake by ENT1 (Nagy et al., 1989, 1990; Choi et al., 2004). Given that ethanol also attenuates evoked DA release in NAc (Yorgason et al., 2014, 2015; Karkhanis et al., 2015; Rose et al., 2016), we tested whether acute ethanol exposure might increase tonic A_1R-mediated inhibition of DA release via impaired ENT1 function. We pre-treated slices with ethanol (2–3 hrs), at a concentration (50 mM) that correlates to a blood alcohol concentration of 230 mg/dl in humans and is

consistent with what late-stage alcoholics achieve (Brick and Erickson, 2009). We first confirmed that pre-treating slices with ethanol using this paradigm reduced $[DA]_o$ evoked by single and five pulses (50 Hz) of electrical stimulation in NAcC (**Figure 6A**, 1p: $t_{(12)} = 2.74$, $p = 0.018$; 5p: $t_{(12)} = 2.67$, $p = 0.020$; unpaired t tests). Next, we found that the effect of A_1R antagonism with CPT (10 µM) on $[DA]_o$ evoked by single electrical pulses was elevated compared to control slices (**Figure 6B**, $F_{(1, 12)} = 18.04$, $p = 0.0011$, two-way RM ANOVA: main effect of drug). A_1 receptor antagonism with CPT decreased the ratio of $[DA]_o$ evoked by 5p:1p (50 Hz) (**Figure 6C**, $F_{(1, 12)} = 68.51$, $p < 0.0001$, two-way RM ANOVA: main effect of drug), and there was a significant interaction between ethanol and CPT (**Figure 6C**, $F_{(1, 12)} = 9.36$, $p = 0.0099$, two-way RM ANOVA: ethanol x CPT interaction), which was borne out by a more pronounced decrease after ethanol than in control slices (**Figure 6D**, $t_{(12)} = 3.16$, $p = 0.0082$, unpaired t test). To test directly whether ethanol in this paradigm impaired adenosine uptake by ENT1, we imaged tonic extracellular adenosine levels with the GRAB-Ado sensor during application of ENT1 inhibitor NBTI (10 µM). NBTI increased tonic extracellular adenosine levels in NAcC to a significantly lesser degree in slices preincubated with ethanol than controls (**Figure 6E**, $F_{(1,17)} = 11.30$, $p = 0.0037$, two-way RM ANOVA: main effect of drug; $t_{(17)} = 2.60$, $p = 0.019$, unpaired t test). These data indicate that tonic A_1R-mediated inhibition of DA axons by adenosine in the NAcC is elevated by acute ethanol exposure, paralleled by an underlying attenuated uptake of adenosine uptake by ENT1.

DISCUSSION (1,636 words)

Here, we reveal that DA release in NAcC is under a tonic inhibition by ambient adenosine levels acting at A_1Rs, and that ENT1, located at least in part on striatal astrocytes, governs the level of this tonic inhibition. Moreover, we reveal that ethanol promotes A_1R-inhibition of DA release, through elevating adenosine levels by diminishing adenosine uptake via ENT1. These data support the emerging concept that astrocytes play important roles in setting the level of striatal DA output, in health and disease.

Direct versus indirect actions of A_1Rs

Our data provide functional evidence for direct regulation of DA release by A_1Rs. Immunocytochemical studies in rat striatal synaptosomes indicate that dopaminergic axons can contain A_1Rs (Borycz et al., 2007), but direct immunocytochemical evidence *in situ* is currently lacking. We excluded indirect actions of A_1Rs via key candidate pathways, namely cholinergic inputs that act via nAChRs and GABAergic networks that act via $GABA_A$/$GABA_B$ receptors on DA axons. Previous reports have excluded effects of glutamatergic modulation (Borycz et al., 2007; O'Connor and O'Neill, 2008). Moreover, we found that A_1R agonists inhibited DA release evoked by even single short optogenetic stimulation of ChR2-expressing DA axons, which should not co-activate other striatal neurons, suggesting that the location(s) for A_1Rs that regulate DA are either a currently undisclosed tonically active cell type with currently unknown actions on DA or, more parsimoniously, DA axons themselves.

Tonic inhibition

A_1R antagonists enhanced DA release evoked by single short optogenetic stimulation, suggesting that A_1R activation does not require stimulation of any other network, and is tonically activated by an ambient striatal adenosine tone. An adenosine tone at striatal A_1Rs has previously been described on glutamate inputs in NAcC (Brundege and Williams, 2002; Choi et al., 2004). Extracellular adenosine concentrations in the brain have been suggested to be in the range of 25–250 nM under basal conditions, which are sufficient to activate high-affinity A_1Rs (Dunwiddie and Masino, 2001). In further support for a resting adenosine tone in NAcC, we could detect extracellular adenosine with the GRAB-Ado sensor, following application of an ENT1 inhibitor, in the absence of any striatal stimulation. The source of adenosine is still undetermined, but can arise from the catabolism of ATP from neuronal and non-neuronal sources (Latini and Pedata, 2008), including astrocytes (Corkrum et al., 2020).

A_1Rs modify DA signal contrast for firing frequency

We found that A_1R activation not only limits the overall amplitude of DA output, but promotes the contrast in DA signals released by different firing rates and pulse numbers, and vice versa, A_1R antagonists reduce this contrast. The strength of A_1R-mediated inhibition of DA release varied with adenosine concentration, resulting from ENT1 inhibition or overexpression, and furthermore, was greater for lower frequencies of activation of DA axons. These data indicate that an adenosine tone preferentially limits DA output during the lower frequencies of DA neuron activity that represent tonic activity, while leaving relatively intact the DA release evoked by the higher frequencies associated with phasic activity in DA neurons. The preferential inhibition of DA release by low frequencies of activity parallels the effects of GABA input to DA axons (Lopes et al., 2019; Roberts et al., 2020; Roberts et al., 2021) and could indicate a preferential influence of striatal adenosine on DA functions that are proposed to be mediated by low frequencies of activity e.g. the ongoing monitoring of reward value and its changes (Wang et al., 2021). We identified an underlying change in the dynamic short-term plasticity (STP) of DA output that corresponds to this change to frequency filtering, that again parallels the effect of GABA on STP in DA release (Lopes et al., 2019; Roberts et al., 2020). Elsewhere in the brain, A_1R activation, including through ambient adenosine, can modulate STP of glutamate transmission through a presynaptic mechanism (Perrier et al., 2019; Qi et al., 2017; Yang et al., 2007; Moore et al., 2003; Wong et al., 2006). A_1Rs are $G_{i/o}$ coupled, and so their activation causes inhibition of adenylyl cyclase, activation of potassium channels and inactivation of voltage-gated calcium channels (VGCCs) (Haas and Selbach, 2000). We have recently revealed that mechanisms that determine axonal excitability, particularly potassium-dependent processes, strongly gate STP of DA release (Condon et al., 2019) while calcium largely gates amplitude. We therefore hypothesise that A_1Rs on striatal DA axons likely inhibit the overall amplitude of DA release via reduced VGCC activity while simultaneously gating the STP of DA release by modifying axonal excitability via potassium-dependent conductances. Future studies are needed to establish these potential mechanisms.

ENT1 and astrocytes are key regulators of tonic A_1R-inhibition of DA release

We established that ENT1 in NAcC limits ambient adenosine levels and tonic A_1R-inhibition of DA axons, and thereby indirectly facilitates DA release. ENT1 usually facilitates adenosine uptake from the extracellular milieu, but can reverse to release adenosine (Parkinson et al., 2011), and ENT1 has been shown to facilitate adenosine release evoked by electrical stimulation in cultured hippocampal neurons (Wu et al., 2020). Intriguingly, we found that adenosine release driven by electrical stimulation was TTX-insensitive and sensitive to ENT1 inhibition. Together, our data show that ambient adenosine in NAcC is limited by uptake via ENT1, but can be released via ENT1 reversal in some conditions. There is an additional ENT in striatum, ENT2 (Jennings et al., 2001; Anderson et al., 2002), whose roles we did not explore. ENT1 is thought to be responsible for the majority of adenosine transport and, subsequently, the key regulator of extracellular adenosine levels across the brain (Young et al., 2008).

We found a major role for ENT1 located to striatal astrocytes, although we did not test or exclude roles for ENT1 located on neurons. The glial metabolic poison fluorocitrate limited the effects of ENT1 inhibitors on adenosine tone, while overexpressing ENT1 in astrocytes boosted evoked DA release by limiting tonic A_1R-inhibition. This strategy for viral overexpression of ENT1 in striatal astrocytes has previously been shown to increase ENT1 expression by ~30%, but also increases striatal GFAP expression and modifies astrocyte morphology (Hong et al., 2020). ENT1 expression has also been shown to regulate astrocyte-specific excitatory amino acid transporter 2 (EAAT2) and aquaporin-4 expression in NAcC (Wu et al., 2010; Lee et al., 2013). These additional astrocyte-specific modifications might also contribute to boosted DA signalling in NAcC, beyond mechanisms involving tonic inhibition by adenosine tone. Regardless, astrocytic ENT1 in striatum has previously been reported to play key roles in reward-seeking behaviours (Hong et al., 2020; Kang et al., 2020), which our data suggest could be mediated by underlying changes to DA signalling.

The role for ENT1 on astrocytes in gating DA output parallels our recent finding that GABA transporters (GAT1 and GAT3) on astrocytes in dorsal striatum set the level of tonic GABAergic inhibition of DA release (Roberts et al., 2020). Furthermore, EAAT2, enriched on astrocytes, limits glutamate-mediated inhibition of DA release (Zhang and Sulzer, 2003), and thus, our collective findings point to astrocytic transporters across neurotransmitter categories as regulators of DA release.

Dysregulation of A_1R-inhibition of DA release by ethanol

To probe the wider potential significance of the regulation of DA in NAcC by adenosine tone and ENT1, we explored whether A_1R inhibition of DA release was modified by ethanol. Ethanol has been shown to increase extracellular adenosine levels by impairing adenosine uptake via ENT1 after acute exposure (Nagy et al., 1989, 1990; Choi et al., 2004), and separately, to reduce DA release following acute application (Yorgason et al., 2014, 2015) or following chronic intermittent exposure in mice (Karkhanis et al., 2015; Rose et al., 2016). Here we bridge these different findings by revealing that ethanol can reduce DA output via a boosted tonic A_1R-inhibition. While pre-treating slices with 50 mM ethanol to understand disruption to cellular and circuit function has limitations in informing effects on behaviour, we speculate that this mechanism could help to explain how striatal A_1Rs contribute to the ataxic and hypnotic effects of ethanol (Meng and Dar, 1995; Phan et

al., 1997; Dar, 2001), as well as how acute ethanol exposure attenuates concurrent GABA co-release from DA axons in dorsal striatum (Kim et al., 2015).

Chronic ethanol exposure is thought to evoke an adaptive response, resulting in decreased ENT1 expression, and therefore a reduced ability for ethanol to increase extracellular adenosine (Nagy et al., 1989). Indeed, rats permitted daily access to ethanol for 8 weeks exhibit downregulated ENT1 gene expression in NAc (Bell et al., 2009). ENT1-null mice exhibit reduced hypnotic and ataxic responses to ethanol, increased ethanol consumption, and decreased adenosine tone in NAc, while viral-mediated rescue of ENT1 expression in NAc reduces ethanol consumption (Choi et al., 2004; Jia et al., 2020). Furthermore, growing evidence implicates striatal adenosine signalling in the neurobiological adaptations of other drugs of abuse (Bachtell, 2017; Ballesteros-Yáñez et al., 2018). Repeated cocaine administration enhances adenosine uptake, reduces adenosine tone, and reduces plasma membrane A_1R expression in NAcC (Manzoni et al., 1998; Toda et al., 2003), while striatal μ-opioid receptor activation by opioids results in reduced striatal adenosine tone in dorsomedial striatum (Adhikary and Birdsong, 2021). Dysregulated tonic A_1R-inhibition of glutamate afferents in NAc is thought to be a key circuit adaptation underlying ethanol abuse and other drugs of abuse (Choi et al., 2004; Chen et al., 2010; Wu et al., 2010; Nam et al., 2011); however, given the role adenosine tone plays in setting the level and activity-dependence of DA output we describe here, we speculate that dysregulated tonic A_1R-inhibition of DA release in NAcC might also be an important circuit adaptation underlying drug abuse.

In conclusion, we show here that A_1Rs can tonically inhibit DA output though an ambient adenosine tone, and that A_1Rs additionally regulate the activity-sensitivity of DA release, preferentially impacting on release by low frequencies. Furthermore, we find that tonic A_1R-inhibition of DA release is regulated by ENT1 and astrocytes, and dysregulated by ethanol. These data provide a further mechanism through which ethanol modulates striatal DA function, and corroborate emerging data highlighting astrocytic transporters as important regulators of striatal function.

REFERENCES

Adhikary S, Birdsong WT (2021) μ opioid receptors acutely regulate adenosine signaling in a thalamo-striatal circuit. bioRxiv:2021.05.25.445648.

Alexander SP, Reddington M (1989) The cellular localization of adenosine receptors in rat neostriatum. Neuroscience 28:645–651.

Anderson CM, Xiong W, Geiger JD, Young JD, Cass CE, Baldwin SA, Parkinson FE (2002) Distribution of equilibrative, nitrobenzylthioinosine-sensitive nucleoside transporters (ENT1) in brain. J Neurochem 73:867–873.

Bachtell RK (2017) Cocaine addiction and adenosine A1 and A2A receptors. In: The neuroscience of cocaine: mechanisms and treatment, pp 429–437. Elsevier Inc.

534 Ballesteros-Yáñez I, Castillo CA, Merighi S, Gessi S (2018) The role of adenosine receptors in psychostimulant
535 addiction. Front Pharmacol 8:985.

536 Bell RL, Kimpel MW, McClintick JN, Strother WN, Carr LG, Liang T, Rodd ZA, Mayfield RD, Edenberg HJ, McBride
537 WJ (2009) Gene expression changes in the nucleus accumbens of alcohol-preferring rats following
538 chronic ethanol consumption. Pharmacol Biochem Behav 94:131–147.

539 Boddum K, Jensen TP, Magloire V, Kristiansen U, Rusakov DA, Pavlov I, Walker MC (2016) Astrocytic GABA
540 transporter activity modulates excitatory neurotransmission. Nat Commun 7:13572.

541 Bonansco C, Couve A, Perea G, Ferradas CA, Roncagliolo M, Fuenzalida M (2011) Glutamate released
542 spontaneously from astrocytes sets the threshold for synaptic plasticity. Eur J Neurosci 33:1483–1492.

543 Borycz J, Pereira MF, Melani A, Rodrigues RJ, Köfalvi A, Panlilio L, Pedata F, Goldberg SR, Cunha RA, Ferré S
544 (2007) Differential glutamate-dependent and glutamate-independent adenosine A_1 receptor-mediated
545 modulation of dopamine release in different striatal compartments. J Neurochem 101:355–363.

546 Brick J, Erickson CK (2009) Intoxication is not always visible: an unrecognized prevention challenge. Alcohol Clin
547 Exp Res 33:1489–1507.

548 Britt JP, McGehee DS (2008) Presynaptic opioid and nicotinic receptor modulation of dopamine overflow in the
549 nucleus accumbens. J Neurosci 28:1672–1681.

550 Brown SJ, James S, Reddington M, Richardson PJ (1990) Both A1 and A2a purine receptors regulate striatal
551 acetylcholine release. J Neurochem 55:31–38.

552 Brundege JM, Williams JT (2002) Differential modulation of nucleus accumbens synapses. J Neurophysiol
553 88:142–151.

554 Chai H, Diaz-Castro B, Shigetomi E, Monte E, Octeau JC, Yu X, Cohn W, Rajendran PS, Vondriska TM,
555 Whitelegge JP, Coppola G, Khakh BS (2017) Neural circuit-specialized astrocytes: transcriptomic,
556 proteomic, morphological, and functional evidence. Neuron 95:531-549.

557 Cheffer A, Castillo ARG, Corrêa-Velloso J, Gonçalves MCB, Naaldijk Y, Nascimento IC, Burnstock G, Ulrich H
558 (2018) Purinergic system in psychiatric diseases. Mol Psychiatry 23:94–106.

559 Chen J, Nam HW, Lee MR, Hinton DJ, Choi S, Kim T, Kawamura T, Janak PH, Choi DS (2010) Altered
560 glutamatergic neurotransmission in the striatum regulates ethanol sensitivity and intake in mice lacking
561 ENT1. Behav Brain Res 208:636–642.

562 Choi DS, Cascini MG, Mailliard W, Young H, Paredes P, McMahon T, Diamond I, Bonci A, Messing RO (2004) The
563 type 1 equilibrative nucleoside transporter regulates ethanol intoxication and preference. Nat Neurosci
564 7:855–861.

565 Condon MD, Platt NJ, Zhang YF, Roberts BM, Clements MA, Vietti-Michelina S, Tseu MY, Brimblecombe KR,
566 Threlfell S, Mann EO, Cragg SJ (2019) Plasticity in striatal dopamine release is governed by release-
567 independent depression and the dopamine transporter. Nat Commun 10:1–15.

568 Corkrum M, Covelo A, Lines J, Bellocchio L, Pisansky M, Loke K, Quintana R, Rothwell PE, Lujan R, Marsicano G,
569 Martin ED, Thomas MJ, Kofuji P, Araque A (2020) Dopamine-evoked synaptic regulation in the nucleus
570 accumbens requires astrocyte activity. Neuron 105:1036-1047.

571 Dar MS (2001) Modulation of ethanol-induced motor incoordination by mouse striatal A1 adenosinergic
572 receptor. Brain Res Bull 55:513–520.

573 Dunwiddie T V., Masino SA (2001) The role and regulation of adenosine in the central nervous system. Annu
574 Rev Neurosci 24:31–55.

575 Ferré S, O'Connor WT, Svenningsson P, Björklund L, Lindberg J, Tinner B, Strömberg I, Goldstein M, Ögren SO,
576 Ungerstedt U, Fredholm BB, Fuxe K (1996) Dopamine D1 receptor-mediated facilitation of GABAergic
577 neurotransmission in the rat strioentppeduncular pathway and its modulation by adenosine A1 receptor-
578 mediated mechanisms. Eur J Neurosci 8:1545–1553.

579 Haas HL, Selbach O (2000) Functions of neuronal adenosine receptors. Naunyn Schmiedebergs Arch Pharmacol
580 362:375–381.

581 Hartung H, Threlfell S, Cragg SJ (2011) Nitric oxide donors enhance the frequency dependence of dopamine
582 release in nucleus accumbens. Neuropsychopharmacology 36:1811–1822.

583 Henneberger C, Papouin T, Oliet SHR, Rusakov DA (2010) Long-term potentiation depends on release of d-
584 serine from astrocytes. Nature 463:232–236.

585 Hong S, Bullert A, Baker M, Choi D (2020) Astrocytic equilibrative nucleoside transporter type 1 upregulations
586 in the dorsomedial and dorsolateral striatum distinctly coordinate goal-directed and habitual ethanol-
587 seeking behaviours in mice. Eur J Neurosci:ejn.14752.

588 Jennings LL, Hao C, Cabrita MA, Vickers MF, Baldwin SA, Young JD, Cass CE (2001) Distinct regional distribution
589 of human equilibrative nucleoside transporter proteins 1 and 2 (hENT1 and hENT2) in the central
590 nervous system. Neuropharmacology 40:722–731.

591 Jia YF, Vadnie CA, Ho AMC, Peyton L, Veldic M, Wininger K, Matveyenko A, Choi DS (2020) Type 1 equilibrative
592 nucleoside transporter (ENT1) regulates sex-specific ethanol drinking during disruption of circadian
593 rhythms. Addict Biol 25:e12801.

594 Jones IW, Paul Bolam J, Wonnacott S (2001) Presynaptic localisation of the nicotinic acetylcholine receptor β2
595 subunit immunoreactivity in rat nigrostriatal dopaminergic neurones. J Comp Neurol. 439:235–247.

596 Kang S, Hong SI, Lee J, Peyton L, Baker M, Choi S, Kim H, Chang SY, Choi DS (2020) Activation of astrocytes in
597 the dorsomedial striatum facilitates transition from habitual to goal-directed reward-seeking behavior.
598 Biol Psychiatry 88:797–808.

599 Karkhanis AN, Rose JH, Huggins KN, Konstantopoulos JK, Jones SR (2015) Chronic intermittent ethanol
600 exposure reduces presynaptic dopamine neurotransmission in the mouse nucleus accumbens. Drug
601 Alcohol Depend 150:24–30.

602 Kim JI, Ganesan S, Luo SX, Wu YW, Park E, Huang EJ, Chen L, Ding JB (2015) Aldehyde dehydrogenase 1a1
603 mediates a GABA synthesis pathway in midbrain dopaminergic neurons. Science 350:102–106.

604 Kosillo P, Zhang Y-F, Threlfell S, Cragg SJ (2016) Cortical control of striatal dopamine transmission via striatal
605 cholinergic interneurons. Cereb Cortex 26:4160–4169.

606 Latini S, Pedata F (2008) Adenosine in the central nervous system: release mechanisms and extracellular
607 concentrations. J Neurochem 79:463–484.

608 Lee MR, Ruby CL, Hinton DJ, Choi S, Adams CA, Young Kang N, Choi DS (2013) Striatal adenosine signaling
609 regulates EAAT2 and astrocytic AQP4 expression and alcohol drinking in mice.
610 Neuropsychopharmacology 38:437–445.

611 Lemos JC, Shin JH, Alvarez VA (2019) Striatal cholinergic interneurons are a novel target of corticotropin
612 releasing factor. J Neurosci 39:5647–5661.

613 Lopes EF, Roberts BM, Siddorn RE, Clements MA, Cragg SJ (2019) Inhibition of nigrostriatal dopamine release
614 by striatal GABA A and GABA B receptors. J Neurosci 39:1058–1065.

615 Manzoni O, Pujalte D, Williams J, Bockaert J (1998) Decreased presynaptic sensitivity to adenosine after
616 cocaine withdrawal. J Neurosci 18:7996–8002.

617 Melchior JR, Ferris MJ, Stuber GD, Riddle DR, Jones SR (2015) Optogenetic versus electrical stimulation of
618 dopamine terminals in the nucleus accumbens reveals local modulation of presynaptic release. J
619 Neurochem 134:833–844.

620 Meng Z-H, Dar MS (1995) Possible role of striatal adenosine in the modulation of acute ethanol-induced motor
621 incoordination in rats. Alcohol Clin Exp Res 19:892–901.

622 Moore KA, Nicoll RA, Schmitz D (2003) Adenosine gates synaptic plasticity at hippocampal mossy fiber
623 synapses. Proc Natl Acad Sci U S A 100:14397–14402.

624 Nagai K, Nagasawa K, Fujimoto S (2005) Transport mechanisms for adenosine and uridine in primary-cultured
625 rat cortical neurons and astrocytes. Biochem Biophys Res Commun 334:1343–1350.

626 Nagy LE, Diamond I, Casso DJ, Franklin C, Gordon AS (1990) Ethanol increases extracellular adenosine by
627 inhibiting adenosine uptake via the nucleoside transporter. J Biol Chem 265:1946–1951.

628 Nagy LE, Diamond I, Collier K, Lopez L, Ullman B, Gordon AS (1989) Adenosine is required for ethanol-induced
629 heterologous desensitization. Mol Pharmacol 36:744–748.

630 Nam HW, Lee MR, Zhu Y, Wu J, Hinton DJ, Choi S, Kim T, Hammack N, Yin JCP, Choi DS (2011) Type 1
631 equilibrative nucleoside transporter regulates ethanol drinking through accumbal N-methyl-D-aspartate
632 receptor signaling. Biol Psychiatry 69:1043–1051.

633 Nguyen MD, Ross AE, Ryals M, Lee ST, Venton BJ (2015) Clearance of rapid adenosine release is regulated by
634 nucleoside transporters and metabolism. Pharmacol Res Perspect 3:1–12.

635 Nolan SO, Zachry JE, Johnson AR, Brady LJ, Siciliano CA, Calipari ES (2020) Direct dopamine terminal regulation

by local striatal microcircuitry. J Neurochem 155:475–493.

O'Connor J, O'Neill C (2008) A role for adenosine A1 receptors in GABA and NMDA-receptor mediated modulation of dopamine release: studies using fast cyclic voltammetry. Sensors 8:5516–5534.

O'Neill C, Nolan BJ, Macari A, O'Boyle KM, O'Connor JJ (2007) Adenosine A1 receptor-mediated inhibition of dopamine release from rat striatal slices is modulated by D1 dopamine receptors. Eur J Neurosci 26:3421–3428.

Okada M, Mizuno K, Kaneko S (1996) Adenosine A1 and A2 receptors modulate extracellular dopamine levels in rat striatum. Neurosci Lett 212:53–56.

Pajski ML, Venton BJ (2010) Adenosine release evoked by short electrical stimulations in striatal brain slices is primarily activity dependent. ACS Chem Neurosci 1:775–787.

Parkinson FE, L. Damaraju V, Graham K, Y.M. Yao S, A. Baldwin S, E. Cass C, D. Young J (2011) Molecular biology of nucleoside transporters and their distributions and functions in the brain. Curr Top Med Chem 11:948–972.

Paulsen RE, Contestabile A, Villani L, Fonnum F (1987) An In vivo model for studying function of brain tissue temporarily devoid of glial cell metabolism: the use of fluorocitrate. J Neurochem 48:1377–1385.

Peng L, Huang R, Yu ACH, Fung KY, Rathbone MP, Hertz L (2005) Nucleoside transporter expression and function in cultured mouse astrocytes. Glia 52:25–35.

Peng W, Wu Z, Song K, Zhang S, Li Y, Xu M (2020) Regulation of sleep homeostasis mediator adenosine by basal forebrain glutamatergic neurons. Science 369.

Perrier SP, Gleizes M, Fonta C, Nowak LG (2019) Effect of adenosine on short-term synaptic plasticity in mouse piriform cortex in vitro: adenosine acts as a high-pass filter. Physiol Rep 7:e13992.

Phan TA, Gray AM, Nyce JW (1997) Intrastriatal adenosine A1 receptor antisense oligodeoxynucleotide blocks ethanol-induced motor incoordination. Eur J Pharmacol 323:R5–R7.

Preston Z, Lee K, Widdowson L, Freeman TC, Dixon AK, Richardson PJ (2009) Adenosine receptor expression and function in rat striatal cholinergic interneurons. Br J Pharmacol 130:886–890.

Qi G, Van Aerde K, Abel T, Feldmeyer D (2017) Adenosine differentially modulates synaptic transmission of excitatory and inhibitory microcircuits in layer 4 of rat barrel cortex. Cereb Cortex 27:4411–4422.

Quarta D, Borycz J, Solinas M, Patkar K, Hockemeyer J, Ciruela F, Lluis C, Franco R, Woods AS, Goldberg SR, Ferré S (2004a) Adenosine receptor-mediated modulation of dopamine release in the nucleus accumbens depends on glutamate neurotransmission and N-methyl-D-aspartate receptor stimulation. J Neurochem 91:873–880.

Quarta D, Ferré S, Solinas M, You ZB, Hockemeyer J, Popoli P, Goldberg SR (2004b) Opposite modulatory roles for adenosine A1 and A2A receptors on glutamate and dopamine release in the shell of the nucleus accumbens. Effects of chronic caffeine exposure. J Neurochem 88:1151–1158.

Rice ME, Cragg SJ (2004) Nicotine amplifies reward-related dopamine signals in striatum. Nat Neurosci 7:583–584.

Rice ME, Patel JC, Cragg SJ (2011) Dopamine release in the basal ganglia. Neuroscience 198:112–137.

Richardson PJ, Brown SJ (1987) ATP release from affinity-purified rat cholinergic nerve terminals. J Neurochem 48:622–630.

Roberts BM, Doig NM, Brimblecombe KR, Lopes EF, Siddorn RE, Threlfell S, Connor-Robson N, Bengoa-Vergniory N, Pasternack N, Wade-Martins R, Magill PJ, Cragg SJ (2020) GABA uptake transporters support dopamine release in dorsal striatum with maladaptive downregulation in a parkinsonism model. Nat Commun 11:1–17.

Roberts BM, Lopes EF, Cragg SJ (2021) Axonal modulation of striatal dopamine release by local γ-aminobutyric acid (GABA) signalling. Cells 10:709.

Rose JH, Karkhanis AN, Chen R, Gioia D, Lopez MF, Becker HC, McCool BA, Jones SR (2016) Supersensitive kappa opioid receptors promotes ethanol withdrawal-related behaviors and reduce dopamine signaling in the nucleus accumbens. Int J Neuropsychopharmacol 19:pyv127.

Ross AE, Venton BJ (2015) Adenosine transiently modulates stimulated dopamine release in the caudate-putamen via A1 receptors. J Neurochem 132:51–60.

Solinas M, Ferré S, You ZB, Karcz-Kubicha M, Popoli P, Goldberg SR (2002) Caffeine induces dopamine and glutamate release in the shell of the nucleus accumbens. J Neurosci 22:6321–6324.

Song WJ, Tkatch T, Surmeier DJ (2000) Adenosine receptor expression and modulation of Ca2+ channels in rat striatal cholinergic interneurons. J Neurophysiol 83:322–332.

Stouffer MA, Woods CA, Patel JC, Lee CR, Witkovsky P, Bao L, Machold RP, Jones KT, de Vaca SC, Reith MEA, Carr KD, Rice ME (2015) Insulin enhances striatal dopamine release by activating cholinergic interneurons and thereby signals reward. Nat Commun 6:8543.

Sulzer D, Cragg SJ, Rice ME (2016) Striatal dopamine neurotransmission: Regulation of release and uptake. Basal Ganglia 6:123–148.

Tanaka A, Nishida K, Okuda H, Nishiura T, Higashi Y, Fujimoto S, Nagasawa K (2011) Peroxynitrite treatment reduces adenosine uptake via the equilibrative nucleoside transporter in rat astrocytes. Neurosci Lett 498:52–56.

Threlfell S, Lalic T, Platt NJ, Jennings K a, Deisseroth K, Cragg SJ (2012) Striatal dopamine release is triggered by synchronized activity in cholinergic interneurons. Neuron 75:58–64.

Toda S, Alguacil LF, Kalivas PW (2003) Repeated cocaine administration changes the function and subcellular distribution of adenosine A1 receptor in the rat nucleus accumbens. J Neurochem 87:1478–1484.

Wang Y, Toyoshima O, Kunimatsu J, Yamada H, Matsumoto M (2021) Tonic firing mode of midbrain dopamine neurons continuously tracks reward values changing moment-by-moment. eLife 10:e63166.

Wong AYC, Billups B, Johnston J, Evans RJ, Forsythe ID (2006) Endogenous activation of adenosine A1 receptors, but not P2X receptors, during high-frequency synaptic transmission at the calyx of held. J Neurophysiol 95:3336–3342.

Wu J, Lee MR, Choi S, Kim T, Choi D-S (2010) ENT1 regulates ethanol-sensitive EAAT2 expression and function in astrocytes. Alcohol Clin Exp Res 34:1110–1117.

Wu Z, Cui Y, Wang H, Song K, Yuan Z, Dong A, Wu H, Wan Y, Pan S, Peng W, Jing M, Xu M, Luo M, Li Y (2020) A GRAB sensor reveals activity-dependent non-vesicular somatodendritic adenosine release. bioRxiv:2020.05.04.075564.

Yang SC, Chiu TH, Yang HW, Min MY (2007) Presynaptic adenosine A1 receptors modulate excitatory synaptic transmission in the posterior piriform cortex in rats. Brain Res 1156:67–79.

Yorgason JT, Ferris MJ, Steffensen SC, Jones SR (2014) Frequency-dependent effects of ethanol on dopamine release in the nucleus accumbens. Alcohol Clin Exp Res 38:438–447.

Yorgason JT, Rose JH, McIntosh JM, Ferris MJ, Jones SR (2015) Greater ethanol inhibition of presynaptic dopamine release in C57BL/6J than DBA/2J mice: Role of nicotinic acetylcholine receptors. Neuroscience 284:854–864.

Young JD, Yao SYM, Sun L, Cass CE, Baldwin SA (2008) Human equilibrative nucleoside transporter (ENT) family of nucleoside and nucleobase transporter proteins. Xenobiotica 38:995–1021.

Zhang H, Sulzer D (2003) Glutamate spillover in the striatum depresses dopaminergic transmission by activating group I metabotropic glutamate receptors. J Neurosci 23:10585–10592.

Zhang H, Sulzer D (2004) Frequency-dependent modulation of dopamine release by nicotine. Nat Neurosci 7:581–582.

Table 1. Comparison of effects of adenosine A_1 receptor agonists and antagonists on evoked mean peak $[DA]_o$ between sexes

Sex	Mean $[DA]_o$ (% pre-drug)	SEM	n	unpaired t test
Figure 1B: A_1 agonist (CPA), electrically-evoked DA release				
Male	39.6	6.8	3	$t_{(4)} = 0.467$, $p = 0.665$
Female	43.2	3.9	3	
Figure 1G: A_1 agonist (CPA), optogenetically-evoked DA release				
Male	59.4	2.9	4	$t_{(6)} = 1.141$, $p = 0.297$
Female	53.4	4.4	4	
Figure 3A: A_1 antagonist (CPT), electrically-evoked DA release				
Male	140.8	7.8	4	$t_{(5)} = 0.181$, $p = 0.864$
Female	142.6	5.4	3	
Figure 3C: A_1 antagonist (Caffeine), electrically-evoked DA release				
Male	117.4	8.0	3	$t_{(4)} = 0.304$, $p = 0.777$
Female	114.9	2.2	3	
Figure 3E: A_1 antagonist (CPT), optogenetically-evoked DA release				
Male	126.6	16.7	3	$t_{(6)} = 0.258$, $p = 0.805$
Female	130.0	3.8	5	

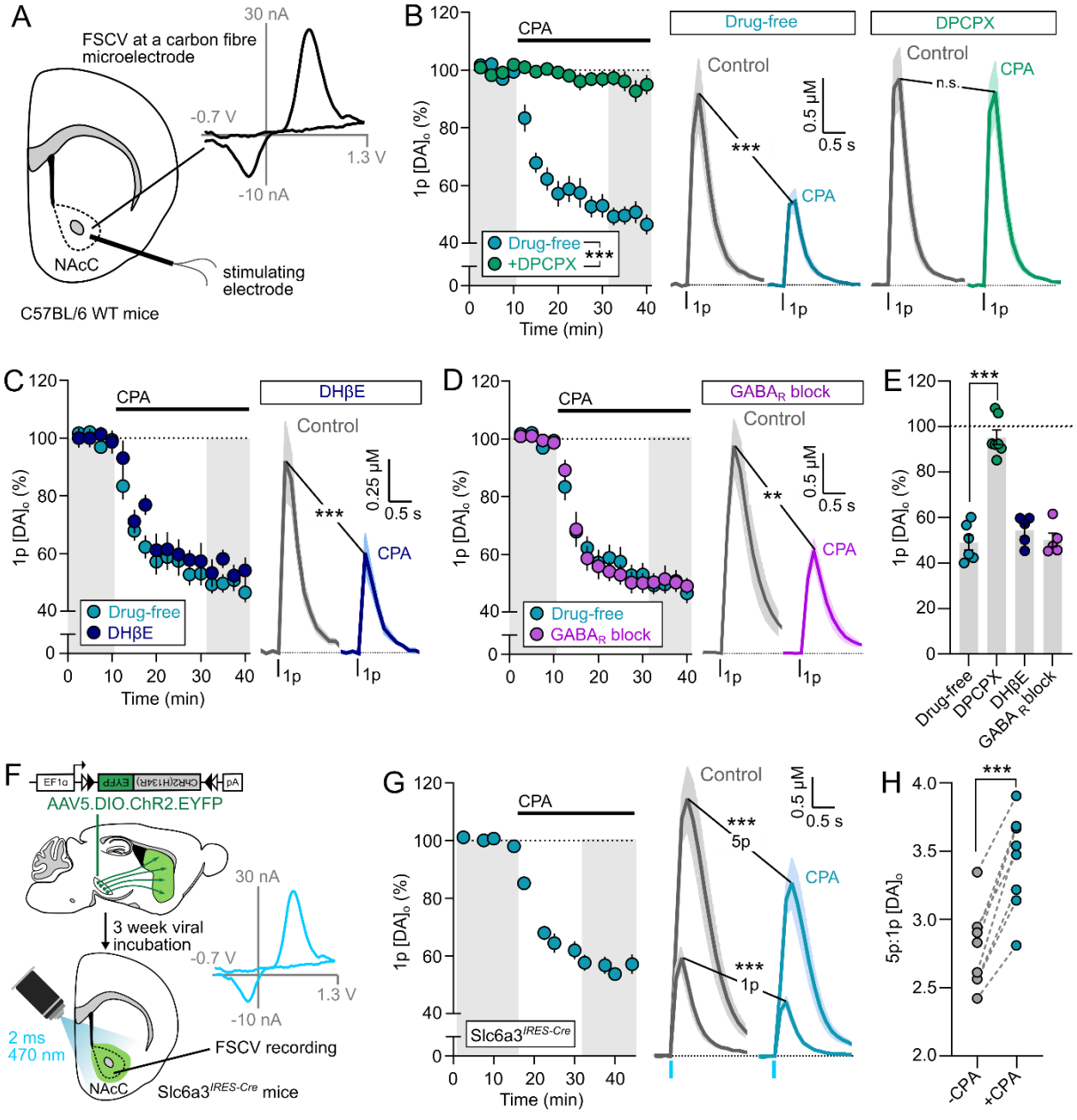

Figure 1. Adenosine A_1R agonists inhibit DA release in NAcC. **A**, Experimental setup for FSCV for DA detection in wild-type mouse NAcC in acute slices. Inset, typical evoked DA voltammogram. **B-D**, Left, Summary of mean peak $[DA]_o$ evoked by a single electrical pulse (1p) before and after application of A_1R agonist CPA (15 µM) normalised to pre-drug baseline (dotted line). Shaded areas represent time points used to obtain data on right, mean $[DA]_o$ transients in either drug-free ACSF (blue *n* = 6 experiments/4 mice), or in the presence of A_1R antagonist DPCPX (2 µM) (B, green, *n* = 8 experiments/5 mice), or nAChR antagonist DHβE (1 µM) (C, dark blue, *n* = 5 experiments/4 mice), or $GABA_A$ and $GABA_B$ antagonists (+)-bicuculline (10 µM) and CGP 55845 (4 µM) (D, purple, *n* = 5 experiments/4 mice). Control data in (C) and (D) are from (B). **E**, Mean peak $[DA]_o$ following application of CPA (15 µM) (as a % of pre-drug baseline, data summarised from (B-D)). **F**, Viral injection into midbrain of Slc6a3$^{IRES\text{-}Cre}$ mice for expression of ChR2-eYFP in DA axons for optogenetic-evoked DA

release. **G**, As in (B) but $[DA]_o$ evoked optogenetically by single light pulses (1p) or five pluses of light (5p) at 25 Hz (n = 8 experiments/5 mice). **H**, Ratio of peak $[DA]_o$ evoked by 5p:1p at 25 Hz before (grey) and after (blue) application of CPA (15 µM). Statistics: ***p<0.001, paired t tests (B,C,D,G,H), unpaired t tests (E) and two-way repeated measures ANOVA (B,C,D). Error bars indicate SEM.

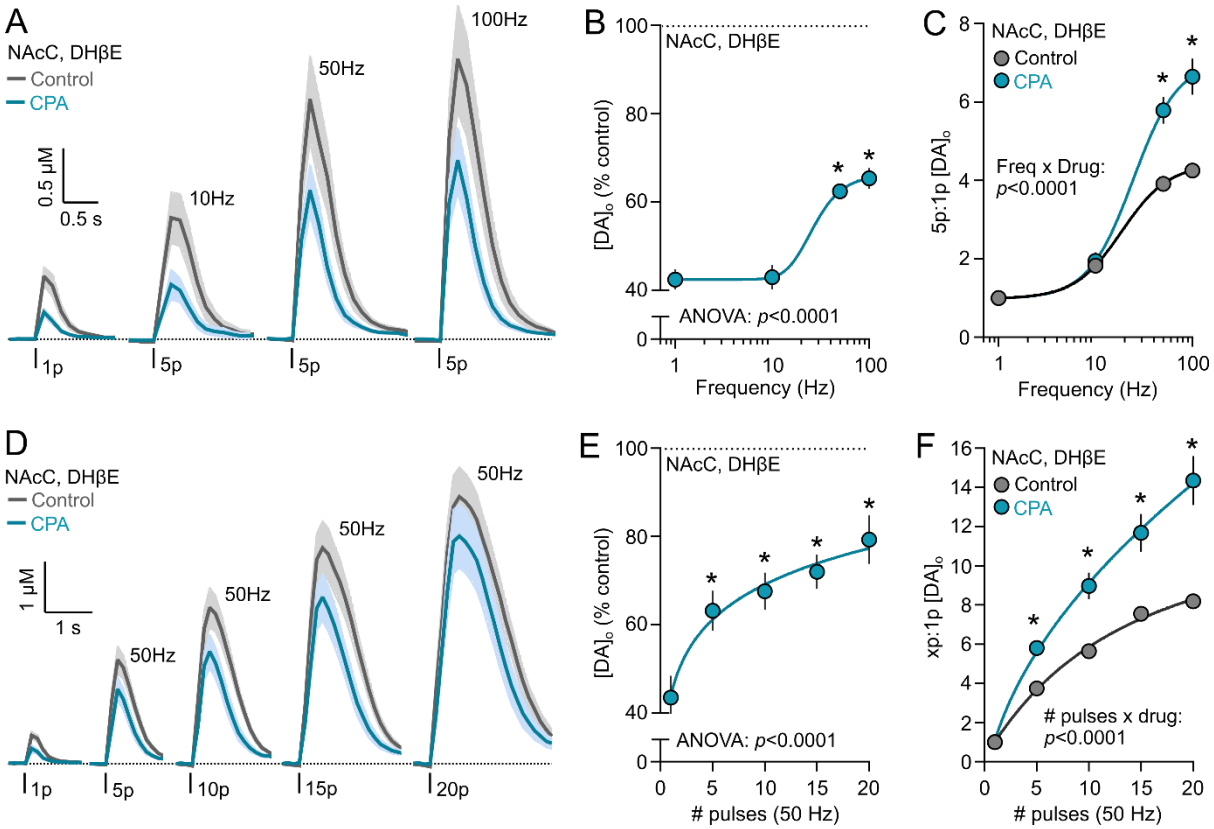

Figure 2. Adenosine A_1R agonists modify the frequency- and activity-sensitivity of DA release in NAcC. A, Mean $[DA]_o$ transients evoked by 1 or 5 electrical pulses in control conditions (grey) or in A_1R agonist CPA (15 µM) (blue) in NAcC (n = 7 experiments/5 mice). **B**, Mean peak $[DA]_o$ from (A) normalised to control conditions versus stimulation frequency. **C**, Mean peak $[DA]_o$ from (A) normalised to 1p in each condition versus stimulation frequency. **D**, Mean $[DA]_o$ transient evoked by 1-20 pulses (50 Hz) of electrical trains in control conditions (grey) or in A_1R agonist CPA (15 µM) (blue) in NAcC (n = 7 experiments/5 mice). **E**, Mean peak $[DA]_o$ from (D) normalised to control conditions versus pulse number. **F**, Mean peak $[DA]_o$ from (D) normalised to 1p in each condition versus number of pulses. Statistics: *p < 0.001, one-way repeated measures ANOVA with Sidak's multiple comparisons to 1p (B,E), two-way repeated measures ANOVA with Sidak's multiple comparisons (C,F). Sigmoidal non-linear curve fits. Error bars indicate SEM. DHβE (1 µM) present throughout.

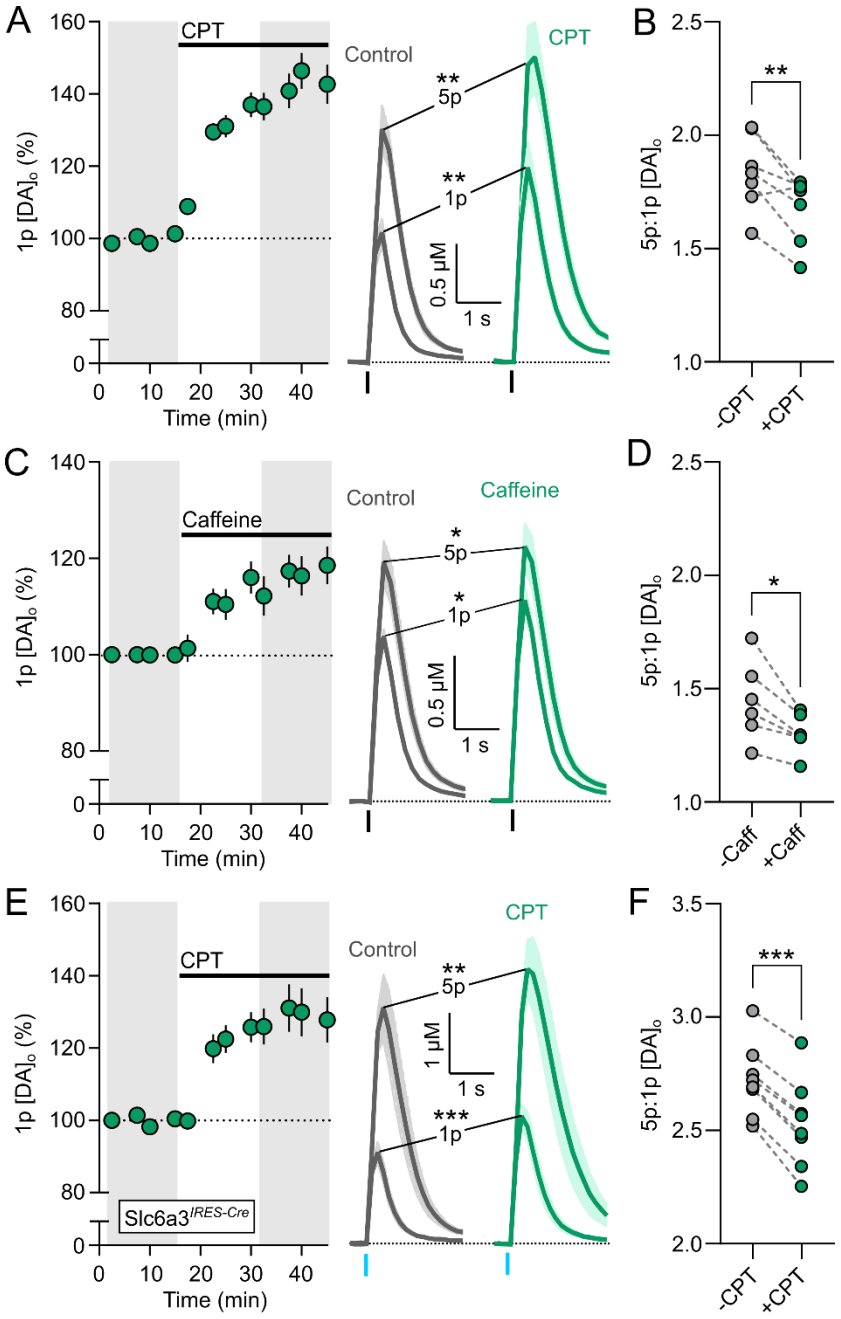

Figure 3. Adenosine A_1R antagonists enhance DA release and correspondingly reduce the activity-sensitivity of DA release in NAcC. A, Left, summary of mean peak $[DA]_o$ before (grey) and after application of A_1R antagonist CPT (10 µM) (green) normalised to pre-drug baseline (dotted line) and right, corresponding mean $[DA]_o$ transients evoked by a single electrical pulse (1p) and five pulses (5p) at 50 Hz in NAcC (n = 7 experiments/4 mice). Shaded areas are used to obtain illustrated transients of $[DA]_o$ and for statistical comparisons. **B**, Ratio of peak $[DA]_o$ evoked by 5p:1p at 50 Hz before (grey) and after (blue) application of CPT (10 µM). Data summarised from (A). **C-D**, As in (A-B) but before (grey) and after application caffeine (20 µM) (green) (n = 6 experiments/4 mice). **E-F**, As in (A-B) but $[DA]_o$ evoked optogenetically by single light pulses (1p) or five pulses (5p) of light at 25 Hz in $Slc6a3^{IRES-Cre}$ mice (n = 8 experiments/5 mice). Statistics: *p<0.05, **p<0.01, ***p<0.001, Paired t tests. Error bars indicate SEM.

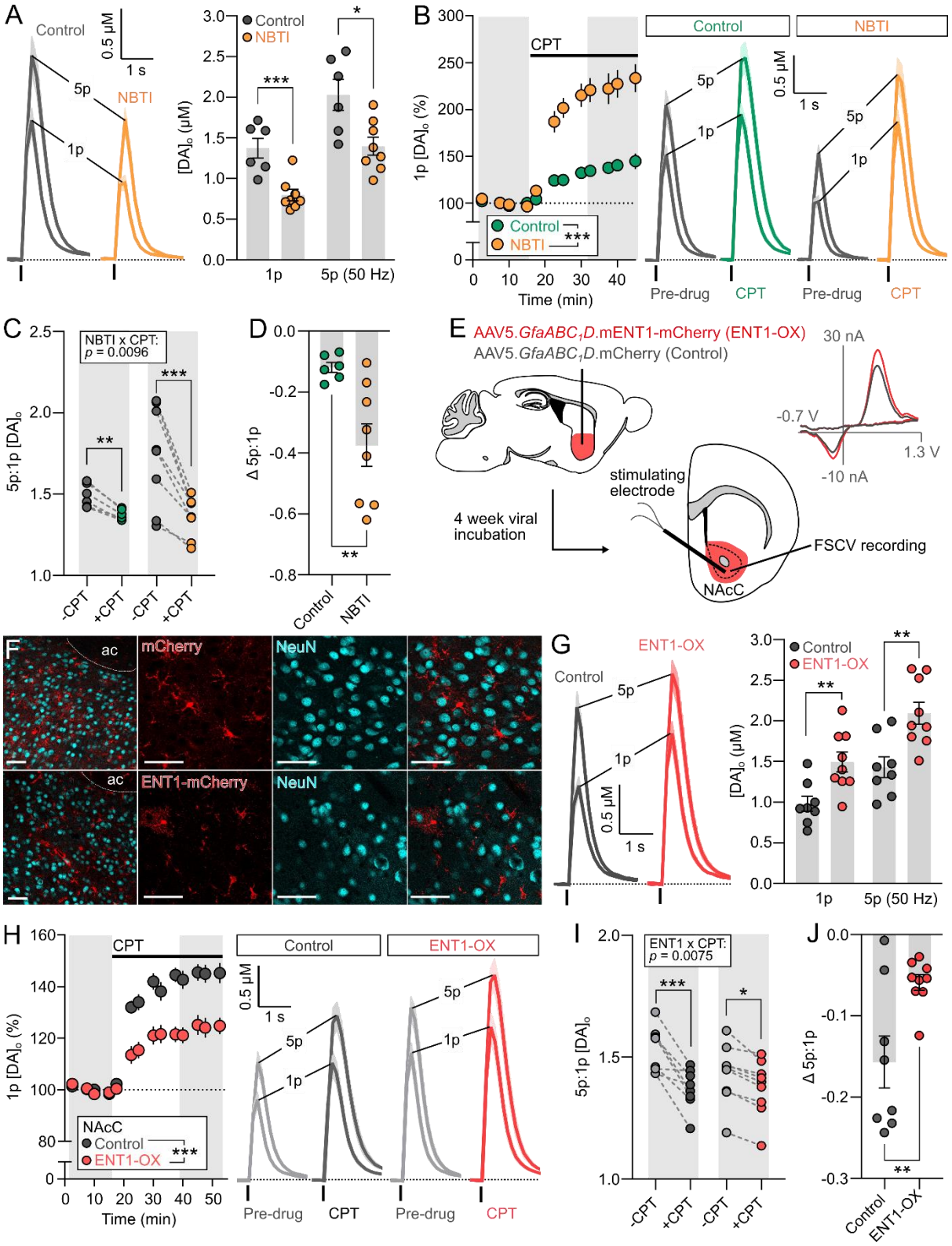

Figure 4. Adenosine uptake by ENT1 on striatal astrocytes regulates tonic A_1R-mediated inhibition of DA release. A, Mean $[DA]_o$ transients (left) and corresponding mean peak $[DA]_o$ (right) evoked by a single electrical pulse (1p) or five pulses (5p) at 50 Hz in NAcC in the absence (grey; *n* = 6 experiments/5 mice) or presence of ENT1 inhibitor NBTI (10 µM) (orange; *n* = 8 experiments/5 mice). **B**, Summary of mean peak $[DA]_o$ before (grey) and after application of A_1R antagonist CPT (10 µM) normalised to pre-drug baseline (dotted line) (left) and right, corresponding mean $[DA]_o$ transients evoked by a single electrical pulse (1p) and five pulses (5p) at 50 Hz in NAcC in the absence (green, *n* = 6 experiments/5 mice) or presence of ENT1 inhibitor NBTI (10 µM) (orange; *n* = 8 experiments/5 mice). **C-D**, Ratio of peak $[DA]_o$ evoked by 5p:1p at 50 Hz (C) and Δ 5p/1p (D) before (grey) and after application of CPT (10 µM) in absence (left, green) or presence of ENT1

inhibitor NBTI (10 µM) (right, orange). Data summarised from (B). **E**, Delivery to NAcC of viral fluorescence-tagged ENT1 driven by an astrocytic promoter to test impact of increased astrocyte-specific expression of ENT1 on DA release detected locally in NAcC. **F**, Immunofluorescence for mCherry (top, red), mCherry-tagged ENT1 (bottom, red) and neuronal marker NeuN (cyan) in NAcC. Scale bars: 40 µm. ac, anterior commissure. **G**, Mean $[DA]_o$ transients (left) and corresponding mean peak $[DA]_o$ (right) evoked by a single electrical pulse (1p) or five pulses (5p) at 50 Hz in NAcC in slices overexpressing ENT1 (ENT1-OX; red; *n* = 9 experiments/4 mice) or expressing control fluorophore mCherry (dark grey; *n* = 8 experiments/4 mice) under an astrocyte-specific promoter. **H**, Summary of mean peak $[DA]_o$ before (grey) and after application of A_1R antagonist CPT (10 µM) normalised to pre-drug baseline (dotted line) (left) and right, corresponding mean $[DA]_o$ transients evoked by a single electrical pulse (1p) and five pulses (5p) at 50 Hz in NAcC in slices overexpressing ENT1 (ENT1-OX; red; *n* = 9 experiments/4 mice) or expressing control fluorophore mCherry (dark grey; *n* = 8 experiments/4 mice). **I**-**J**, Ratio of peak $[DA]_o$ evoked by 5p:1p at 50 Hz (I) and Δ 5p:1p (J) before (light grey) and after application of CPT (10 µM) in slices overexpressing ENT1 (right, red) or expressing control fluorophore mCherry (left, dark grey). Data summarised from (H). Statistics: $p<0.05$, $^{**}p<0.01$, $^{***}p<0.001$, unpaired *t* test (A,D,G,J), two-way repeated measures ANOVA (B,C,H,I) with Sidak multiple comparisons (C,I). Error bars indicate SEM.

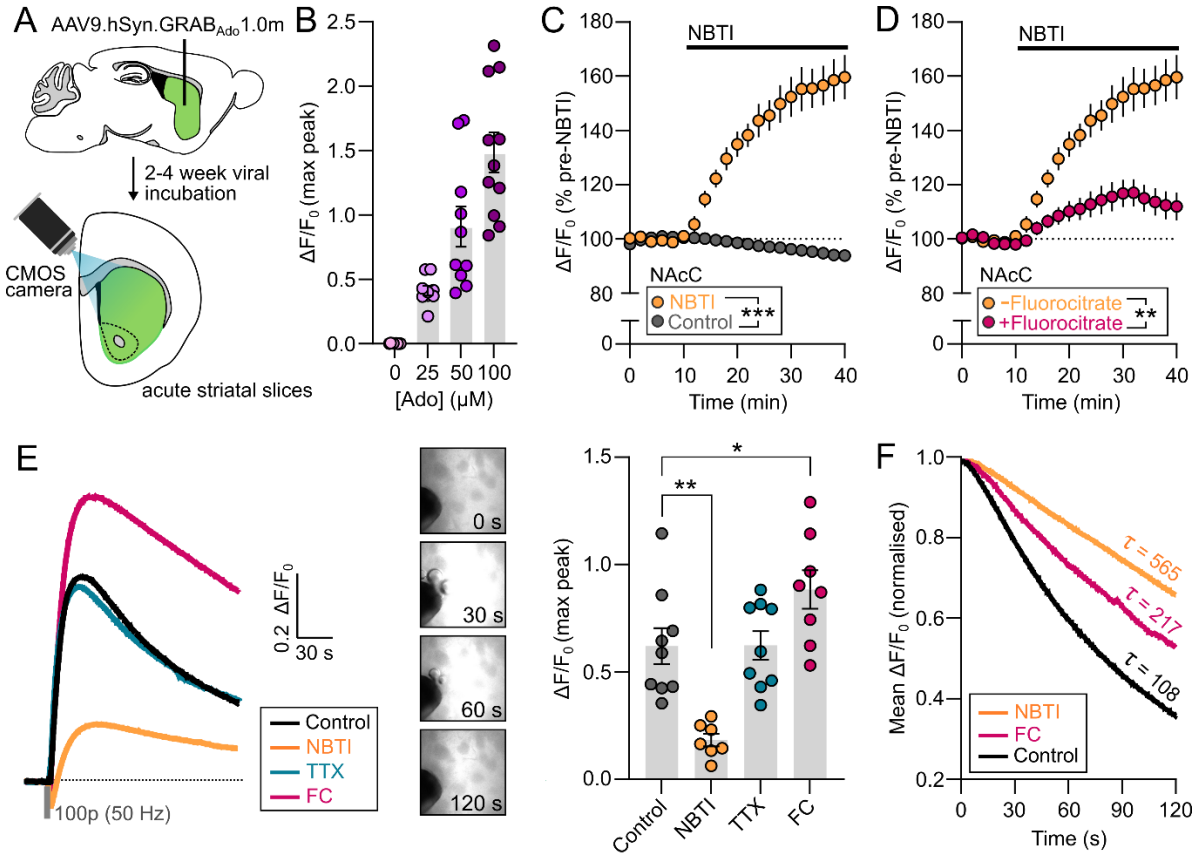

Figure 5. Striatal adenosine tone is regulated by ENT1 activity on striatal astrocytes. **A**, Viral delivery of GRAB-Ado to striatum for imaging extracellular adenosine levels *ex vivo* in acute striatal slices. **B**, Peak $\Delta F/F_0$ in response to increasing concentrations of exogenously applied adenosine (0 – 100 μM) (n = 9 – 11 slices/4 – 6 mice). **C**, Non-stimulated $\Delta F/F_0$ $GRAB_{Ado}$ signal in NAcC normalised to before drug application (dotted line) in control conditions (dark grey, n = 10 experiments/5 mice) or before and after application of NBTI (10 μM) (orange, n = 10 experiments/5 mice). **D**, As in (C) but in the presence of gliotoxin fluorocitrate (100 μM) (pink, n = 6 experiments/ 4 mice). **E**, Mean transients (left) and mean peak (right) $\Delta F/F_0$ $GRAB_{Ado}$ signal evoked by 100 electrical pulses (50 Hz) in drug-free control conditions (n = 9 slices / 5 mice) or the presence of NBTI (10 μM) (orange; n = 7 experiments/5 mice), TTX (1 μM) (blue; n = 9 experiments/5 mice) or fluorocitrate (100 μM) (pink; n = 8 experiments/5 mice). **F**, Mean $\Delta F/F_0$ decay phase normalised to peak from (E). Statistics: *p<0.05, **p<0.01, ***p<0.001, two-way repeated measures ANOVA (C,D), and one-way ANOVA with Sidak multiple comparisons (E). Nonlinear regression with extra-sum-of-squares F test; τ = decay time constant (F). Error bars indicate SEM.

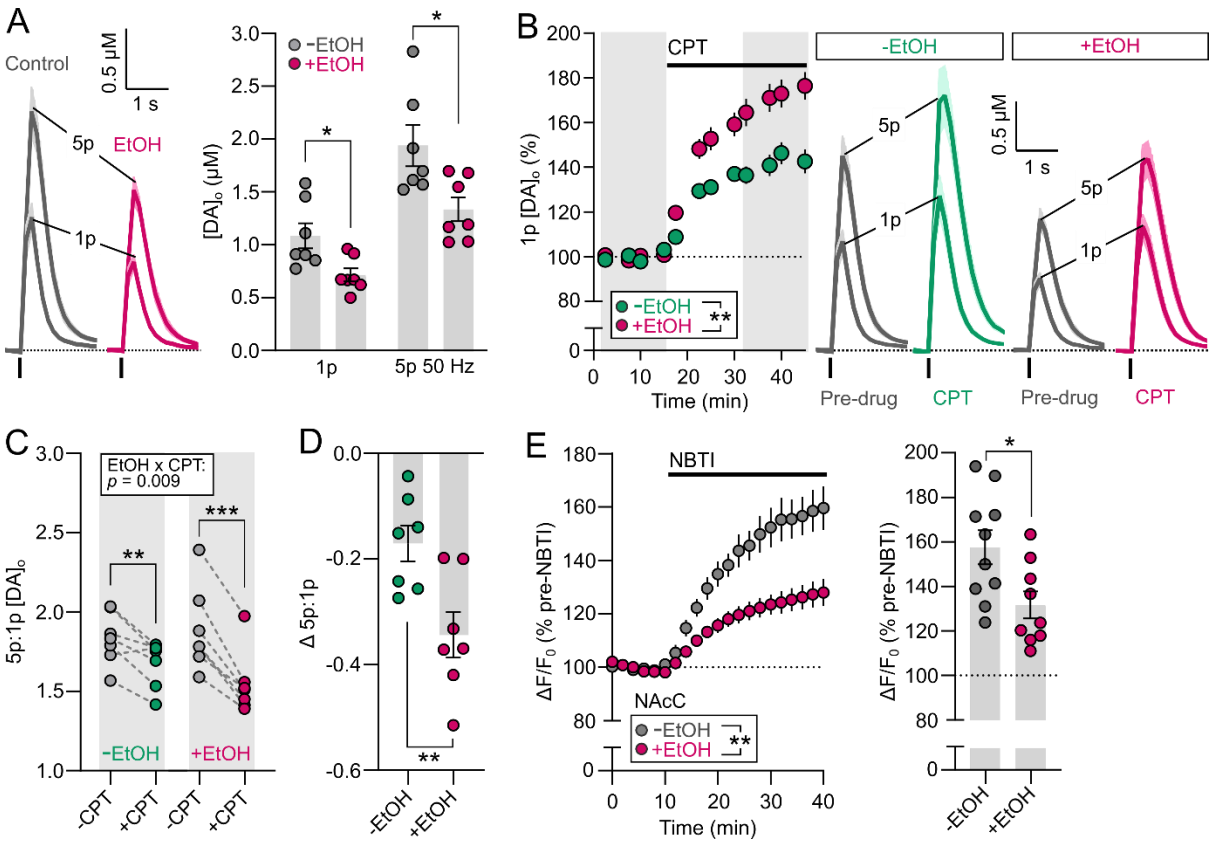

Figure 6. EtOH enhances tonic adenosine A_1R-mediated inhibition of DA release. **A**, Mean $[DA]_o$ transients (left) and corresponding mean peak $[DA]_o$ (right) evoked by a single electrical pulse (1p) or five pulses (5p) at 50 Hz in NAcC in the absence (grey; *n* = 7 experiments/4 mice) or presence of 50 mM EtOH (pink; *n* = 7 experiments/4 mice). **B**, Summary of mean peak $[DA]_o$ before (grey) and after application of A_1R antagonist CPT (10 µM) normalised to pre-drug baseline (dotted line) (left) and right, corresponding mean $[DA]_o$ transients evoked by a single electrical pulse (1p) and five pulses (5p) at 50 Hz in NAcC in the absence (green, *n* = 7 experiments/4 mice) or presence of 50 mM EtOH (pink; *n* = 7 experiments/4 mice). **C-D**, Ratio of peak $[DA]_o$ evoked by 5p:1p at 50 Hz (C) and Δ 5p/1p (D) before (grey) and after application of CPT (10 µM) in absence (left, green) or presence of 50 mM EtOH (right, pink). Data summarised from (B). **E**, Summary (left) and mean peak (right) of unstimulated $\Delta F/F_0$ GRAB-Ado signal in NAcC normalised to pre-drug baseline (dotted line) before and after application of ENT1 inhibitor NBTI (10 µM) in the absence (grey; *n* = 10 experiments/5 mice) or presence of 50 mM EtOH (pink; *n* = 9 experiments/5 mice). Statistics: $p<0.05$, $^{**}p<0.01$, $^{***}p<0.001$, unpaired *t* test (A,D), two-way repeated measures ANOVA (B,C,E) with Sidak multiple comparisons (C). Error bars indicate SEM.

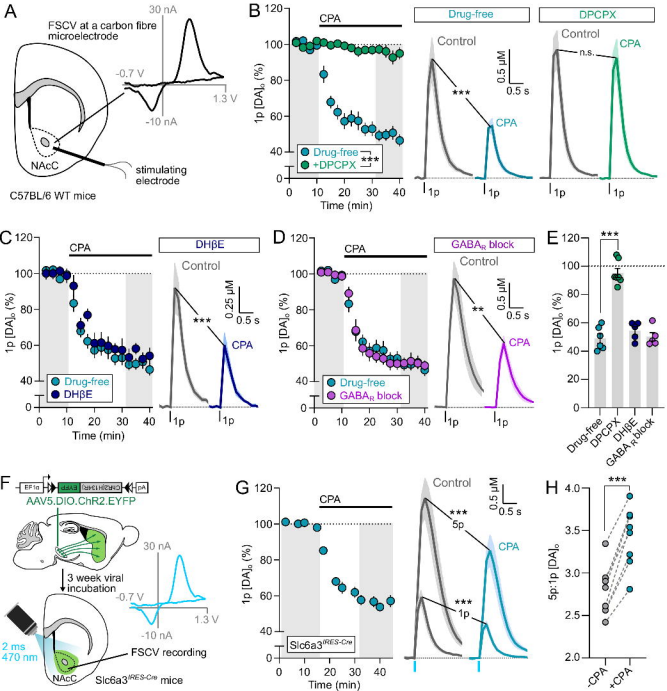
A
30 nA
FSCV at a carbon fibre microelectrode
-0.7 V
1.3 V
-10 nA
NAcc
stimulating electrode
C57BL/6 WT mice
B
CPA
Drug-free
DPCPX
Control
CPA
n.s.
0.5 µM
0.5 s
***
1p [DA]o (%)
Drug-free
+DPCPX
Time (min)
C
CPA
DHβE
Control
0.25 µM
Drug-free
DHβE
Time (min)
D
CPA
GABAB block
Control
**
Drug-free
GABAB block
E
Drug-free
DPCPX
DHβE
GABAB block
F
EF1α
ChR2
SdHG1
WPRE
pA
AAV5.DIO.ChR2.EYFP
3 week viral incubation
30 nA
-0.7 V
1.3 V
-10 nA
2 ms
470 nm
FSCV recording
NAcc
Slc6a3IRES-Cre mice
G
CPA
Control
5p
1p
CPA
Slc6a3IRES-Cre
Time (min)
H
5p:1p [DA]o
-CPA
+CPA

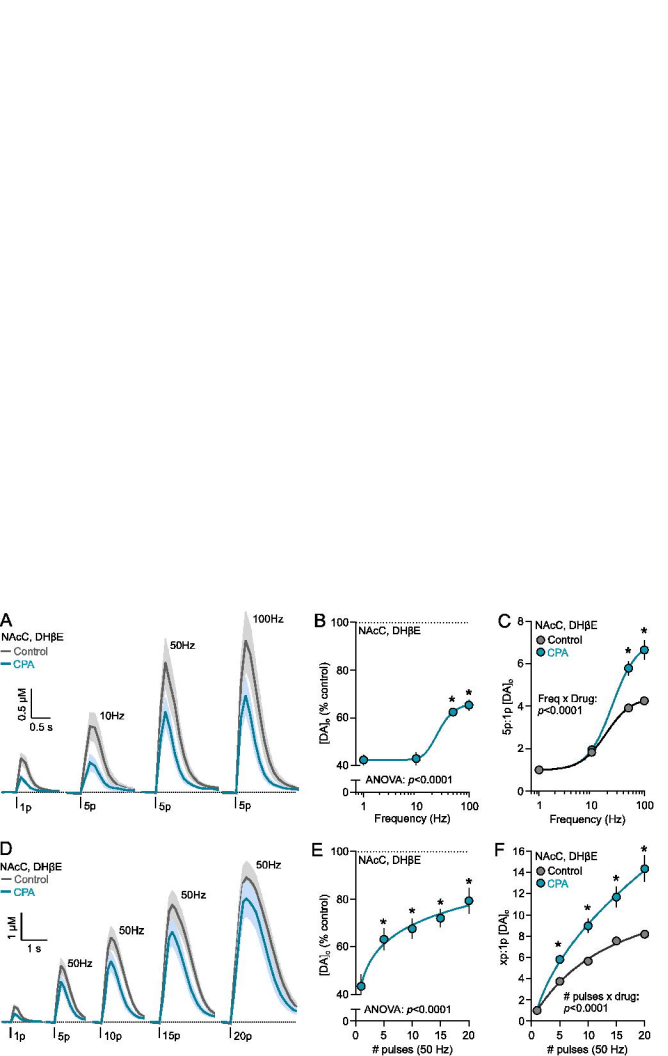
A
NAcC, DHβE
Control
CPA
0.5 μM
0.5 s
100Hz
50Hz
10Hz
1p
5p
5p
5p
B
NAcC, DHβE
[DA]o (% control)
ANOVA: p<0.0001
Frequency (Hz)
C
NAcC, DHβE
Control
CPA
Freq x Drug:
p<0.0001
5p:1p [DA]o
Frequency (Hz)
D
NAcC, DHβE
Control
CPA
1 μM
1 s
50Hz
50Hz
50Hz
50Hz
50Hz
1p
5p
10p
15p
20p
E
NAcC, DHβE
[DA]o (% control)
ANOVA: p<0.0001
pulses (50 Hz)
F
NAcC, DHβE
Control
CPA
pulses x drug:
p<0.0001
xp:1p [DA]o
pulses (50 Hz)

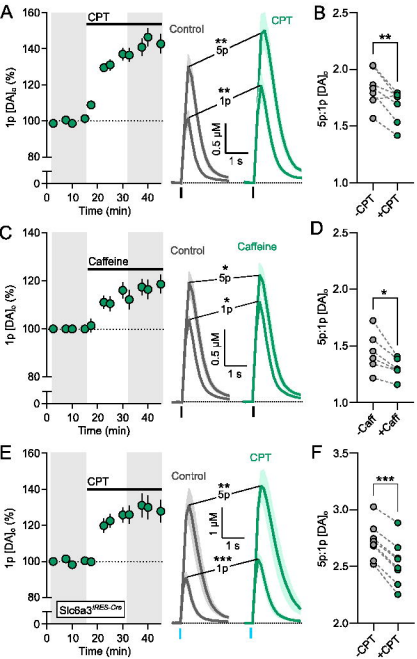
A
CPT
1p [DA]o (%)
Time (min)
Control
CPT
**
5p
**
1p
0.5 µM
1 s
B
5p:1p [DA]o
**
-CPT
+CPT
C
Caffeine
1p [DA]o (%)
Time (min)
Control
Caffeine
*
5p
*
1p
0.5 µM
1 s
D
5p:1p [DA]o
*
-Caff
+Caff
E
CPT
1p [DA]o (%)
Time (min)
Slc6a3 iWES.Cre
Control
CPT
**
5p
1 µM
1 s
***
1p
F
5p:1p [DA]o
***
-CPT
+CPT

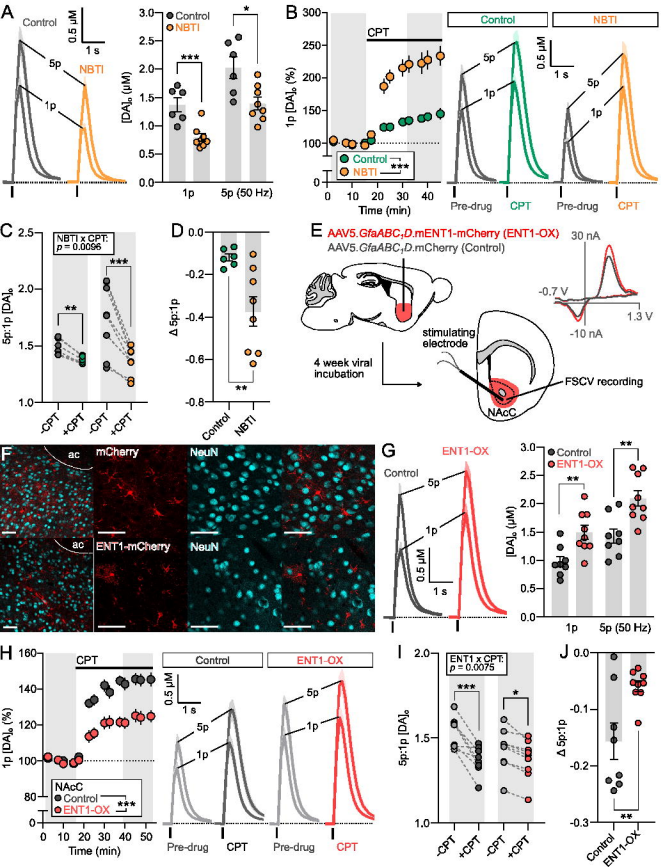
A
Control
NBTI
0.5 µM
1 s
5p
1p
[DA]o (µM)
1p
5p (50 Hz)
***
*
B
CPT
1p [DA]o (%)
Time (min)
Control
NBTI
***
Pre-drug
CPT
C
NBTI x CPT:
p = 0.0096
5p:1p [DA]o
-CPT
+CPT
**
***
D
Δ 5p:1p
Control
NBTI
E
AAV5.GfaABC1D.mENT1-mCherry (ENT1-OX)
AAV5.GfaABC1D.mCherry (Control)
30 nA
-0.7 V
1.3 V
-10 nA
stimulating electrode
4 week viral incubation
FSCV recording
NAcC
F
ac
mCherry
NeuN
ENT1-mCherry
G
ENT1-OX
Control
ENT1-OX
H
NAcC
I
ENT1 x CPT:
p = 0.0075
J

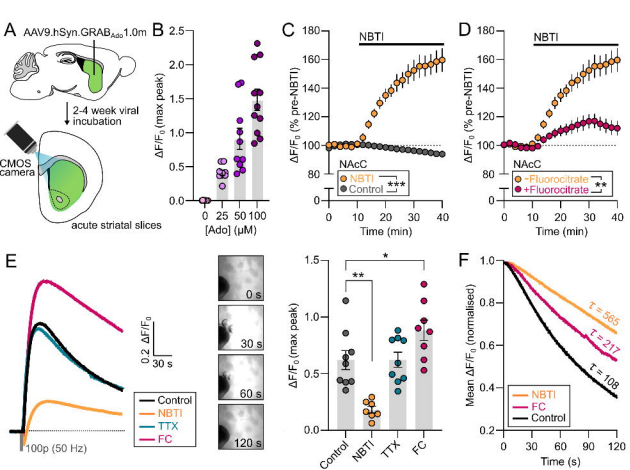
A
AAV9.hSyn.GRAB$_{Ado}$1.0m
2-4 week viral incubation
CMOS camera
acute striatal slices
B
ΔF/F$_0$ (max peak)
[Ado] (μM)
C
NBTI
NAcC
NBTI
Control
***
ΔF/F$_0$ (% pre-NBTI)
Time (min)
D
NBTI
NAcC
-Fluorocitrate
+Fluorocitrate
**
ΔF/F$_0$ (% pre-NBTI)
Time (min)
E
0.2 ΔF/F$_0$
30 s
Control
NBTI
TTX
FC
100p (50 Hz)
0 s
30 s
60 s
120 s
ΔF/F$_0$ (max peak)
Control
NBTI
TTX
FC
F
Mean ΔF/F$_0$ (normalised)
τ = 565
τ = 217
τ = 108
NBTI
FC
Control
Time (s)

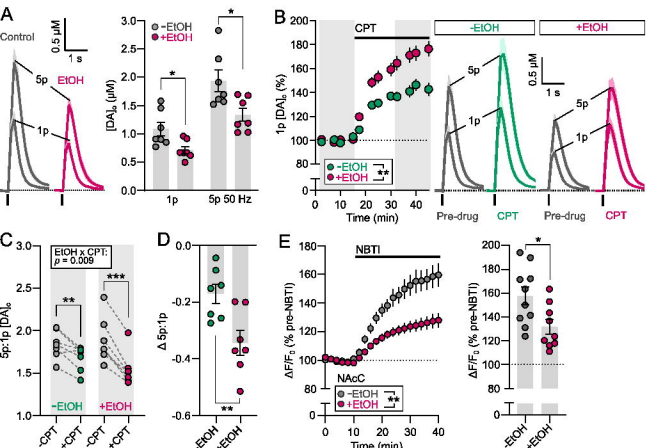
A
Control
0.5 µM
1 s
5p
1p
EtOH
[DA]o (µM)
-EtOH
+EtOH
1p
5p 50 Hz
B
CPT
1p [DA]o (%)
Time (min)
-EtOH
+EtOH
Pre-drug
CPT
C
EtOH x CPT:
p = 0.009
5p:1p [DA]o
-CPT
+CPT
D
Δ 5p:1p
E
NBTI
ΔF/F0 (% pre-NBTI)
NAcC